5-2015

Controls on Dissolution Rate Variation at a Pair of Underflow-Overflow Springs at The Savoy Experimental Watershed

Kiefer Allen Vaughn
University of Arkansas, Fayetteville

Controls On Dissolution Rate Variation At A Pair Of Underflow-Overflow Springs At The Savoy Experimental Watershed

Controls On Dissolution Rate Variation At A Pair Of Underflow-Overflow Springs At The Savoy Experimental Watershed

A thesis submitted in partial fulfillment
of the requirements for the degree of
Master of Science in Geology

by

Kiefer Allen Vaughn
University of Arkansas at Little Rock
Bachelor of Science in Geology, 2012

May 2015
University of Arkansas

This thesis is approved for recommendation to the Graduate Council.

_____
Dr. Matt Covington
Thesis Director

_____
Dr. Ralph K. Davis
Committee Member

_____
Dr. Phillip D. Hays
Committee Member

ABSTRACT

Physical dissolution experiments and numerical modeling have been used in the past to study limestone dissolution rates. Numerical models have typically used constant dissolution rates, whereas rates in nature vary in time. Limestone tablets allow natural estimation of rates over month time scales, but these rates cannot necessarily be extrapolated to geologic timescales and also do not aid our understanding of short term variability. This study characterizes natural variability in these rates and examines potential causes of that variability from first principles. This may enable more accurate projections of dissolution rates within models. This study combines measurement of physical and chemical time series with high-resolution measurements of P_{CO2} at two karst springs within the Savoy Experimental Watershed. These measurements were used to numerically estimate dissolution rates, and these rates were compared against insitu experiments with limestone tablets. This allowed for identification of the potential controlling variables of the dissolution rate at the two karst springs. Modeled dissolution rates for the two springs were strongly correlated with the temporal patterns of P_{CO2}. P_{CO2} was a strong function of surface air temperature. The modeled rates calculated for the sites were then compared with the rate measured from the tablets. This comparison showed that, while the models generally overpredicted the rates, they matched the general trends in dissolution rates over time. The use of high-resolution P_{CO2} monitoring allowed for high resolution modeled dissolution rate calculations. This in turned allowed for dissolution rate characterization that showed how the variability of natural waters effects dissolution rates over time.

TABLE OF CONTENTS

LIST OF FIGURES

LIST OF TABLES

INTRODUCTION

Problem Statement

Physical dissolution experiments and numerical modeling have been used in the past to aid the study of dissolution rates. The physical dissolution experiment that has been extensively used to quantify dissolution rates in karst terrain is weight differencing of limestone tablets (e.g., Trudill, 1975; Gams, 1981; Plan, 2005; Palmer, 2007). This has largely been used to determine relative rates over the period the tablets were exposed. These observed rates could then be extrapolated to obtain long-term solution feature growth estimates. However, this method has a fundamental limitation in that rates observed on a human time scale, e.g. <5 years, might not represent the rates expected over geologic time scales. Also, there are variations that occur during karst feature evolution, such as degassing of carbon dioxide due to enlarging cave entrances (Palmer, 2007). Consequently, karst is not developed in a linear progression but instead in periods of varying progress, with periods of incision through the dissolution process and periods of aggradation through precipitation processes.

Current numerical models of speleogenesis typically employ boundary conditions that assume constant chemical conditions within the inflowing water and constant hydraulic head gradients or discharges across the system (Groves et al., 1999). While an assumption of constant conditions eases calculations of dissolution rates and karst feature evolution, natural waters are not constant with regards to chemical and physical parameters. It would make sense then to look at the variability in terms of the causation of dissolution from first principles in order to more accurately project dissolution rates. Characterizing the variations in dissolution rates and the physical and chemical parameters will allow for more accurate models of karst formation.

Characterization is done through the monitoring of the water chemistry and other relevant parameters over a period of time with high enough resolution to identify trends and patterns within the data. This notion is not new, Groves et al. (2005) collected high-resolution data of both physical and chemical parameters to evaluate the rates of change in the carbonate chemistry and in water/rock interaction at a variety of timescales. The main variables that are to be studied are pH, discharge (Q), specific conductance (SpC), temperature, and dissolved CO_2 concentration. In the past pH, Q, SpC, and temperature could be measured and recorded at high resolution. But, dissolved CO_2 concentration measurements were limited to either spot measurements from grab samples through analysis of a headspace equilibrated with sampled water (Kling et al., 1991; Hope et al., 1995) or indirect estimation from water chemistry calculations that use pH, alkalinity, dissolved ion concentrations, and temperature-dependent equilibrium constants (Stumm and Morgan, 1995, Neal et al., 1998). Each of these methods presents problems when attempting to get high-resolution data. The direct measurement method can use automated water sampling to increase resolution, but this is problematic due to the degassing process once the samples are bottled. The indirect method of measurements is problematic due to the accuracy of the pH measurements; it's possible that small-scale changes might not be observed, due to uncertainty from those measurements (Hach Environmental, 2008, YSI Environmental, 2008). Johnson et al. 2010 developed the solution to these problems that allowed for the direct in situ and continuous measurement of dissolved CO_2 using infrared gas analysis. This method has been used successfully in multiple studies since its inception (Dinsmore et al. 2010, Covington et al. 2013, Dinsmore et al. 2013). This now allows for measurements at high-resolution of all variables of interest for dissolution rate calculations.

Dissolution Rates & CO_2 Dynamics

Dissolution rates are dependent on many variables: the aggressiveness of the water, hydraulics, rock type, and temperature (Palmer, 2009). The aggressiveness of the water refers to the ability of the water to dissolve rock, in our case limestone. The solubility of calcite, the mineral which limestone is composed of, by dissociation in de-ionized water is very low, only 14 mg L^{-1} at 25°C (Ford & Williams, 2007). This in comparison is just slightly more than the solubility of quartz, a seemingly insoluble mineral. In natural waters the solubility of calcite is much higher. As water dissolves carbon dioxide (CO_2) it becomes more acidic by producing carbonic acid (H_2CO_3). This, as a result, is the driving force for enhanced limestone dissolution in natural waters (1). Consequently, CO_2 plays a vital role in the dissolution process.

$$CaCO_3\,(s) + H_2CO_3 \leftrightarrow Ca^{2+} + 2HCO_3^- \qquad (1)$$

The CO_2 that is introduced into the water comes from a variety of CO_2 sources. The most common sources are the atmosphere and soil, either from root respiration or microbial respiration. CO_2 can also be sourced from deep within the Earth, via faults. This type of CO_2 is thought to be from the mantle and/or thermal metamorphism of oceanic carbonate rocks (Sano, 1996). This paper will only consider the more common shallow sources of CO_2. Atmospheric CO_2 is dissolved in water. The equilibrium concentration for CO_2 is reached once the concentration of dissolved gas is proportional to the partial pressure of the gas and the solubility of the gas, as governed by Henry's Law. Currently, atmospheric CO_2 has a concentration of 0.038%, and this equates to a partial pressure CO_2 (P_{CO2}) of 3.8×10^{-4} atm that is available for absorption by the water. If water with higher CO_2 levels is exposed to atmospheric conditions,

the excess P_{CO2} greater than atmospheric levels will be released as equilibrium is restored through the process of degassing. Such elevated CO_2 levels are typically reached as surface water infiltrates through the ground, encountering the soil zone. Soil CO_2 levels are controlled by plant root respiration and microbial activity within the soil and usually range from 0.01 and 0.10 atm (Brooks et al., 1983; Raich and Schlesinger, 1992; Atkin et al., 2000; Ford & Williams, 2007). Soil CO_2 production is highly dependent on surface temperature (Reich & Schlesinger, 1992; Lloyd & Taylor, 1994; 2000; Baldini et al., 2006; Baldini et al., 2008, Knierim, 2009; Palmer, 2009; Yang et al., 2012). This leads to seasonal variations in soil CO_2, with the highest concentrations being in the summer (warmer) months and the lowest being in the winter (cooler) months. Variability is also seen on a diurnal scale in soil and water CO_2 concentrations (Atkin et al., 2000, Dinsmore et al., 2009). With the CO_2 concentrations in the water and soils being higher during the days and lower during the evenings.

Along with CO_2 another factor that can influence dissolution rates is the dissolved load in the water. As the dissolved load of the water increases, the aggressiveness of the water is decreased (Palmer, 1999). This is important in the dissolution rate equation because as the dissolved load increases the constituents of the water will be forced to the point of saturation that effectively stops dissolution. Dissolved load is variable over time as well, a previous study (Whitsett, 2002) at the Savoy Experimental Watershed showed a correlation between discharge and dissolved load. Although other studies have shown that the variation in dissolved ion concentrations in streams is typically small compared to the magnitude of the variation in discharge (Godsey et al., 2008).

Objectives

The purpose of this study is to examine the variability of the chemical and physical parameters of natural karst waters as a controlling factor on dissolution rates. The primary goals of this study are to:

1. Characterize the variability of P_{CO2} in karst springs using high-resolution CO_2 data loggers and identify the primary controls.
2. Characterize the variability of the modeled dissolution rates and identify the primary controls.
3. Compare measured dissolution rates from a physical dissolution experiment with modeled rates that utilize high-resolution water chemistry measurements.

Study Area

The Savoy Experimental Watershed (SEW) is a University of Arkansas owned property encompassing roughly 1250 hectares that lies approximately 24 km west of the main campus in Fayetteville, AR (Fig. 1). It's bound on the north and west by the Ozark National Forest and on the south and east by private livestock farms. The SEW was developed as a long-term field laboratory and is used as an integrated research site at the watershed scale. Evaluating process controls, budgets, modeling, and management practices related to animal production in a mantled karst setting were among the main purposes for its establishment (Brahana et al., 1999). The SEW is within the Springfield Plateau, which is one physiographic provinces of the Ozark Plateau. The area has a temperate climate because of its location at mid-latitude within a continent interior. The mean annual air temperature of the area is 15.5°C (Dugan &

Peckenpaugh, 1985). Average annual precipitation is about 112 cm/yr with the greatest precipitation in late spring (April to June) and least in late winter (December to February).

In the area of the SEW, the Springfield Plateau is characterized by outcrop of the Boone Formation, St. Joe Formation, and the Chattanooga Shale (Fig. 2) These nearly flat-lying formations are thought to have been significantly impacted by reactivated basement faulting associated with the Ouachita orogeny. This basement faulting resulted in orthogonal joint sets in the overlying, brittle carbonate formations. The Boone Formation is a Mississippian-aged fossiliferous limestone interbedded with variable amounts of chert, which increase towards the top of the section (Shelby, 1986). Within the SEW the Boone Formation reaches a maximum thickness of 180 ft. (Al-Rashidy, 1999). The St. Joe Formation is a Mississippian-aged carbonate rock that is a fairly pure limestone. This unit ranges from very thin to over 110 ft. with an average thickness of 20 ft. at the study area (Al-Rashidy, 1999). The Chattanooga Shale is a Devonian-aged fissile shale that has a thickness that averages between 45 and 50 ft. (Unger, 2004) at the SEW. As the Boone Formation weathers, the less soluble chert and clay components of the Formation are left behind to form a regolith layer. This regolith can exceed 150 ft. (Parse, 1995) in thickness in some areas while being less than 5ft or absent on the steeper slopes (Chitsazan, 1980). It averages 45 ft. near the SEW (Laubhan, 2007). This regolith layer is responsible for the slow release of recharge at the SEW that sustains the epikarst springs and the base-flow of Copperhead and Langle Springs.

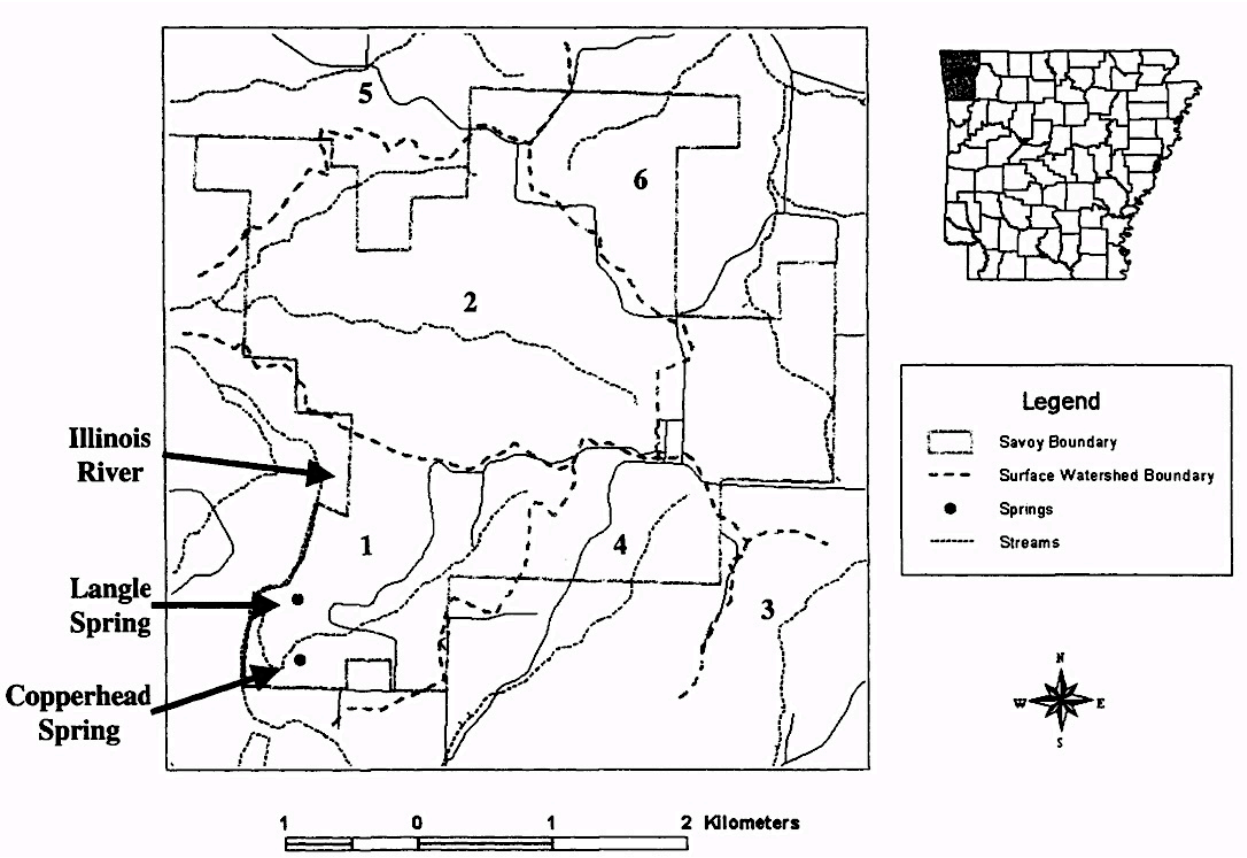

Figure 1. Location of Savoy Experimental Watershed with springs of interest (Whitsett, 2002).

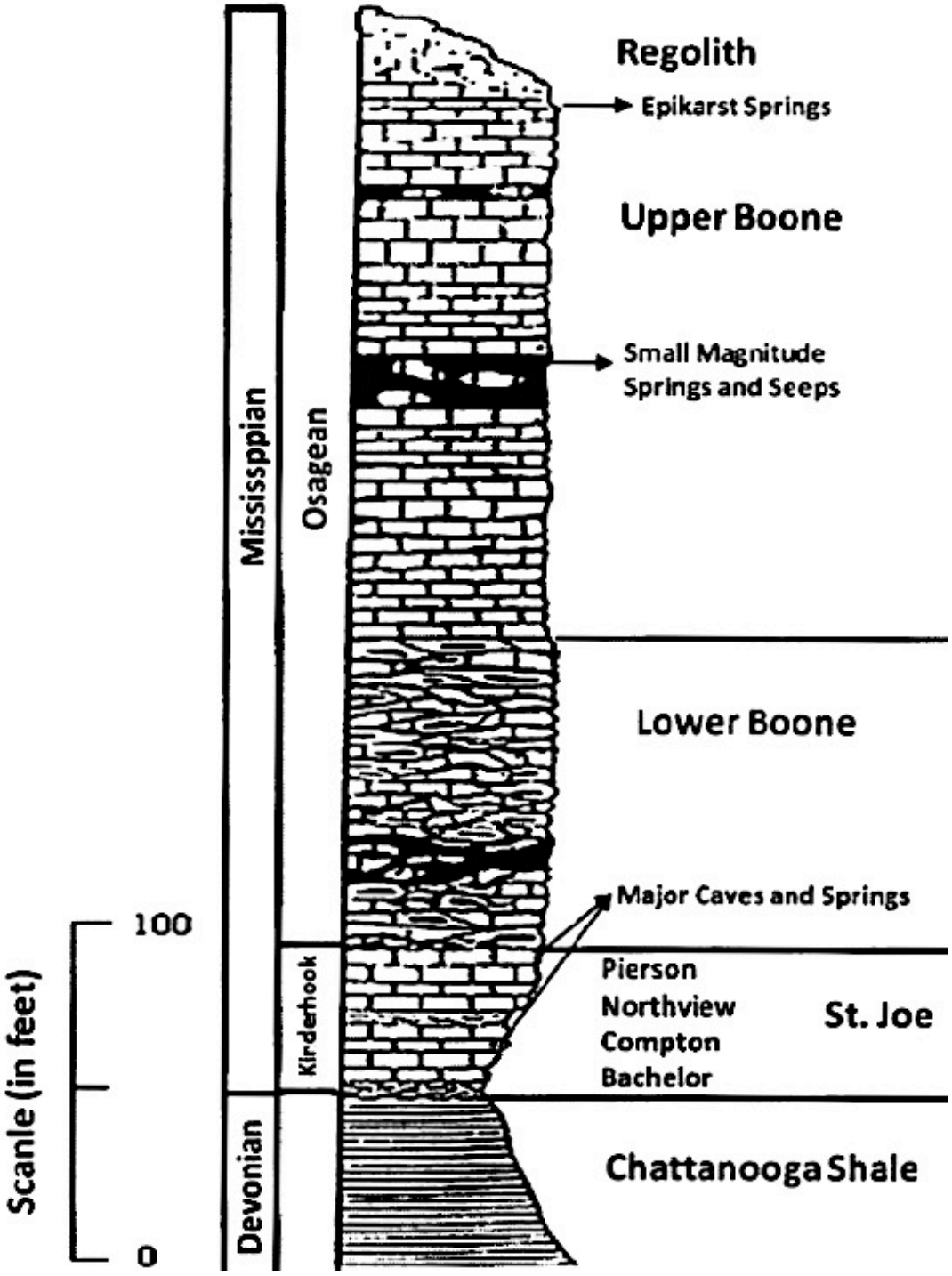

Figure 2. Hydrostratigraphic column of the SEW area (modified from Al-Rashidy, 1999).

Copperhead and Langle Springs

Copperhead and Langle Springs are two of the base-level karst springs located in basin 1 at the SEW. These springs are localized to the area as result of a fault, the Illinois River graben, which forms the western boundary of basin 1. Continuous chert layers within the lower Boone serve as confining layers, perching recharge from above and confining phreatic flow moving up joints that are present within the St. Joe formation (Brahana, 2011). The springs resurge from small caves at the base of the lowermost continuous chert layer in the Boone Formation (Al-Rashidy, 1999).

Although these springs are near to one another and have a similar geological setting they exhibit significant differences in flow characteristics, basin size, geometry of input points/flow-path character, and a different ratio of components that make up their hydrologic budgets (Brahana et al., 1999). Dye traces and continuous flow monitoring at weirs have shown that karst groundwater flow paths and spring basin-size relate to the groundwater levels in basin 1 (Brahana, 2011). These springs are known to be outlets from the same conduit system; Langle with a slightly lower outlet elevation is the underflow spring in the system, while Copperhead with greater permeability at higher elevations is the overflow spring. The dye traces were done at varying flow levels to determine what the sources for each spring were. It was shown that during times of low flow (base-flow) none of the surface-flow appears at Copperhead Spring, it all flows to Langle Spring. Conversely during high flow conditions Copperhead displays a rapid increase in flow and its overall flow is then greater than that of Langle. This relates directly to Langle having a lower resurgence point, capturing a vast majority of the base-flow, while Copperhead is more capable of handling the higher storm flow due to wider openings at higher

elevations. This notion is additionally supported by the fact that there is a small cave at Copperhead (Fig. 3), while Langle does not have an enterable cave system.

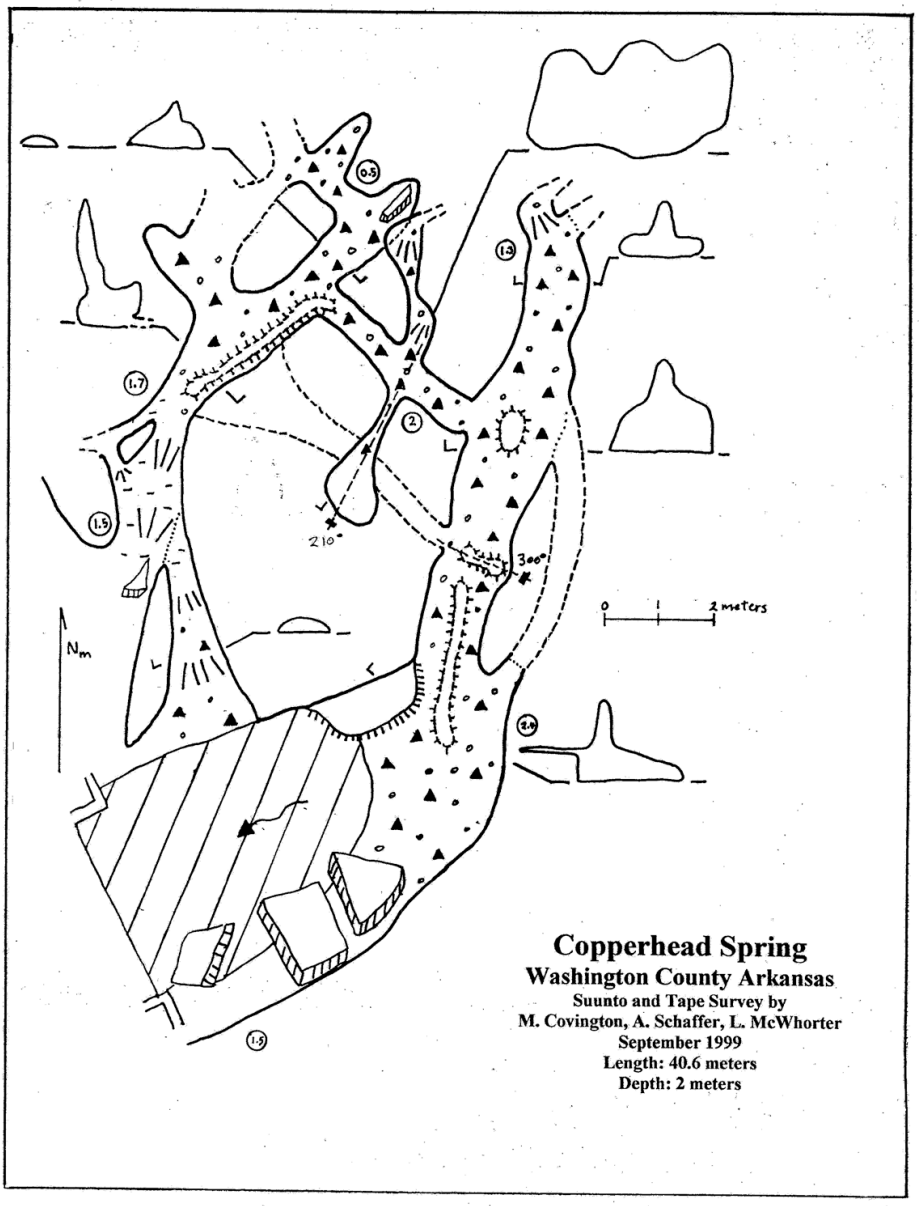

Figure 3. Copperhead Spring cave map (Covington and McWhorter, 1999).

METHODOLOGY

Field Methods

From March 2013 through August 2014 measurements of pH, SpC, stage (height of water in weir), water temperature, and dissolved CO_2 were made at Copperhead and Langle Springs. These were recorded with CR850 Campbell scientific data loggers equipped with a Digital ISFET pH Probe (CS526), electrical conductivity sensor (CS547), pressure transducer (CS451), and a carbon dioxide transmitter (Vaisala, GMT220). The loggers were programmed so that pH, specific conductance, stage, and temperature were recorded at 1-minute resolution, while the CO_2 was recorded at 1.5-hour resolution to reduce power consumption. Air temperature measurements used in this study were from a local airport's (Northwest Arkansas Regional Airport) weather station that is 11.4 miles to the NE of the study area. The stations were fully serviced every three months, which included cleaning and calibration of sensors.

The springs' discharge rates were determined by converting stage measurements using stage-discharge rating curves, Pennington, 2010. These curves were produced using open channel flow equations, weir notch measurements, and corresponding water levels. Weirs were installed at the springs in 1997, through a collaboration of the US Department of Agriculture Agricultural Research Services and US Geological Survey (Brahana personal comm. 2013).

Calibrations of the pH sensor were performed bi-weekly along with the downloading of the data. For quality control and to account for potential sensor drift, spot measurements were collected each time the data was downloaded. These spot field measurements identified potential inconsistencies or drift of the field-deployed sensors. Ultimately, the pH data were discarded as they were determined to be unreliable. Drift in the SpC data was corrected using a linear compensation to match the spot measurements.

Each spring had periods of missing data due to power failure and probe malfunction with Copperhead experiencing this more so than Langle. This was corrected in the latter part of the study with a fortification of the logger's power source. The unreliability of the logger's power seems to have also been the cause of the probe malfunction, as once it was addressed the probes were more reliable.

Physical Installation

The data loggers used in the study were stored in waterproof enclosures in close proximity to the springs allowing for ease of assess during calibration and data collection. The sensors were secured in PVC pipes with cable ties, which allowed for sensor/water interaction with only minimal exposure to damage from debris or unintended jostling. The PVC pipes were secured to rock faces where water levels were high enough for measurements even during low-flow periods.

Direct In-Situ CO_2 Measurements

In order to utilize an atmospheric carbon dioxide transmitter for the purpose of measuring dissolved CO_2 concentrations in water, some modifications were applied (Fig 4). The sensor was enclosed in a protective expanded polytetrafluoroethylen (PTFE) sleeve that is impermeable to water but allowed CO_2 to transfer between water and the sensor. The PTFE was sealed on both ends; this step is vital to the effectiveness of the method and the survival of the sensor. Plasti-Dip was used for this and proved to be effective for the duration of the study. It was important to apply multiple coats of the Plasti-Dip as small holes may have formed due to volatilization during drying process. At least three coats where used on the sensors in the study. Once the sensors were prepared for submersion, they were secured in PVC pipes along with the other

sensors used in the study. This technique is fully described in Johnson et al. 2010, which also included the testing of this method against other CO_2 measurement techniques.

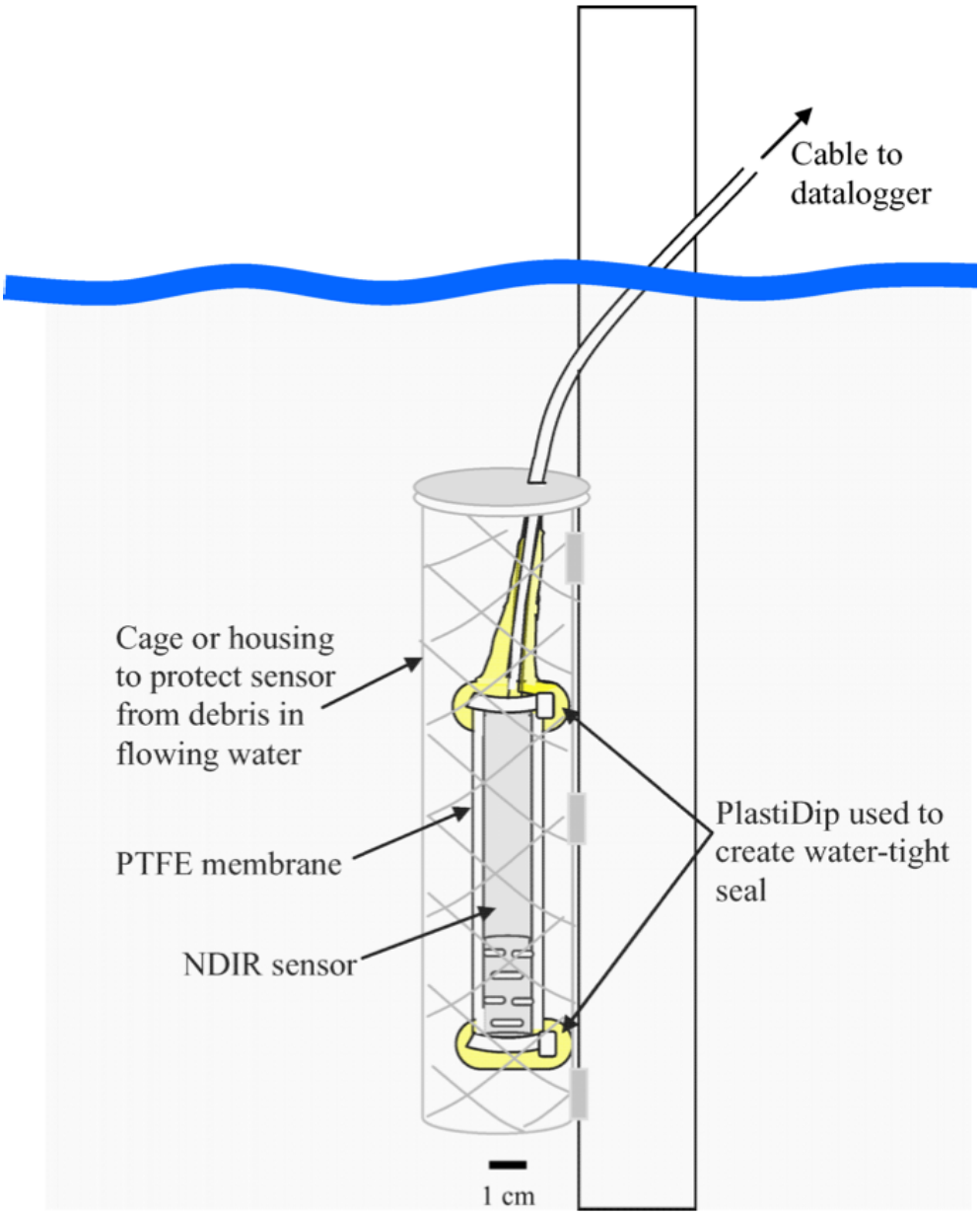

Figure 4. Diagram of Vaisala GMT220 CO_2 sensor deployed in situ. (Johnson et al. 2010)

Physical Dissolution Experiment

A physical dissolution experiment was conducted alongside the continuous measurements of the flow and chemical parameters. This field experiment followed methods from (Trudill, 1975) which used weight loss in limestone tablets to quantify dissolution rates in karstic areas. In this study there were four sets of tablets used. The first three had a three-month residence time (T) in the water, spanning from May 2013 to February 2014, while the last set was in the water from February 2014 to August 2014. The tablets were cored from locally sourced St. Joe limestone; which is a pure phase limestone (Vardy, 2011). The tablets were then etched using a 10% HCL solution for 10 seconds to prepare and clean the tablet surface. The tablets were then dried for 24 hours at a temperature of 100C before being weighed. Once tablets had been dried they were removed from the oven and placed in a desiccator where they were cooled for a one-hour period prior to being weighed. The tablets were weighed twice, and the average of these measurements was used as the pre-exposure weight (W_{pre}) of the tablets. The tablets were then placed in the field by being bolted to the PVC pipe that held the other data logger probes used in the study. This ensured that the tablet and the probes were exposed to the same conditions. To protect the tablets from contact with the pipe and/or bolts/nuts, rubber gaskets were used. Once removed from the field, the tablets were lightly rinsed with tap water as to not further dissolution. They were then dried and the weight was recorded again using the same procedure as the pre-exposure tablets. This weight measured is the post-exposure weight (W_{post}). The radius (r), thickness (t), and the height (h) of each tablet were measured. The thickness was measured at three intervals around the tablet that were then averaged to determine an average thickness. The density (ρ) and surface area (A) were calculated for each tablet by using the equations below:

$$\rho = \frac{m}{V} = \frac{W_{post}}{\pi r^2 t} \qquad (2)$$

$$A = 2\pi r^2 + 2\pi rh \qquad (3)$$

These measurements were then used to calculated the dissolution rates that occurred in the field using the following equation:

$$\text{Dissolution Rate} = \frac{W_{post} - W_{pre}}{T(\text{days})} \times 365 \left(\frac{\text{days}}{\text{yr}}\right) \times \rho^{-1} \times A^{-1} \qquad (4)$$

Analytical methods

Water Samples

As a part of this study a total of seven water samples were collected under a range of flow conditions from both springs between June 2013 and December 2013. These samples were analyzed for Ca^{2+} hardness using the titration method (Hach Method 10253) and were duplicated for quality control. In addition to these samples, data from a previous study spanning from January 2012 to August 2012 (Jarvie personal comm. 2014) were also included to fortify the relationship that was being developed. These measurements were used to create site-specific relationships between SpC and Ca^{2+} concentration. This relationship was compared to the worldwide relationship between SpC and Total Hardness (as mg L^{-1} $CaCO_3$) for karst waters (Krawczyk and Ford, 2006).

Correlations

Correlations coefficients were calculated to help identify potential controls on chemical variability. The Spearman rank-order correlation coefficient (r_s) was used since many of the relationships were non-linear. The Spearman correlation is a nonparametric measure of the monotonicity of the relationship between two datasets. Essentially, r_s quantifies the strength of any type of relationship where values of one variable consistently increase or decrease with another. For this study a significance level of α=0.05 was used.

Dissolution Rate Models

Utilizing logger recorded probe measurement of water temperature, SpC, and dissolved CO_2, dissolution rates for the study period were calculated with a Python package, called olm (Covington et al., in press). The water temperature and dissolved CO_2 data were used directly in the calculations, but the SpC data had to be converted into Ca^{2+} concentrations in order to be utilized. Dissolution rates were calculated using the functions olm.calcite.solutionFromCaPCO2 () and olm.calcite.pwpFromSolution ().

The first step was to obtain a solution object from the Ca^{2+} concentrations, P_{CO2}, and water temperature data using the olm.calcite.solutionFromCaPCO2() function. This function assumes an H_20-CO_2-$CaCO_3$ system. It guesses concentration of H using relaxed charge balance assumption, and iterates to the full solution. Then using a solution object along with P_{CO2} data, a calcite dissolution rate is calculated with the function olm.calcite.pwpFromSolution(). This function uses the PWP (Plummer-Wigley-Parkhurst) (Equation 5).

$$R = k_1 a_{H^+} + k_2 a_{H_2CO_{3^*}} + k_3 a_{H_20} - k_4 a_{Ca^{++}} a_{HCO_{3^-}}, \qquad (5)$$

Where k_i are kinetic coefficients that are a function of temperature and P_{CO2}, and a_x is the activity of ion x (Plummer et al., 1978).

RESULTS

Data at Copperhead and Langle springs were collected from March 3rd, 2013 until August 17th, 2014. Each spring experienced periods of missing data; the most significant loss is CO_2 data at Copperhead from October 2013 through December 2013 and Langle from December 2013 through February 2014. Field measurements were made during this time to provide some sense of conditions during the data gaps. This results section is organized by individual parameters or experiments as to fully describe each.

Water Chemistry

A linear regression was done between Ca^{2+} concentrations and corresponding SpC values measured from water samples at each spring. This gave a linear relationship between the two variables (Fig. 5). This was done to convert SpC measurement taken by the logger in to Ca^{2+} concentrations for use in the dissolution models. Each spring had a unique relationship. To calculate Ca^{2+} concentrations at each spring the following equations were used:

$$Copperhead\ Ca^{2+} = \frac{SpC}{209.42} \qquad (6)$$

$$\text{Langle } Ca^{2+} = \frac{\text{SpC}}{177.51} \qquad (7)$$

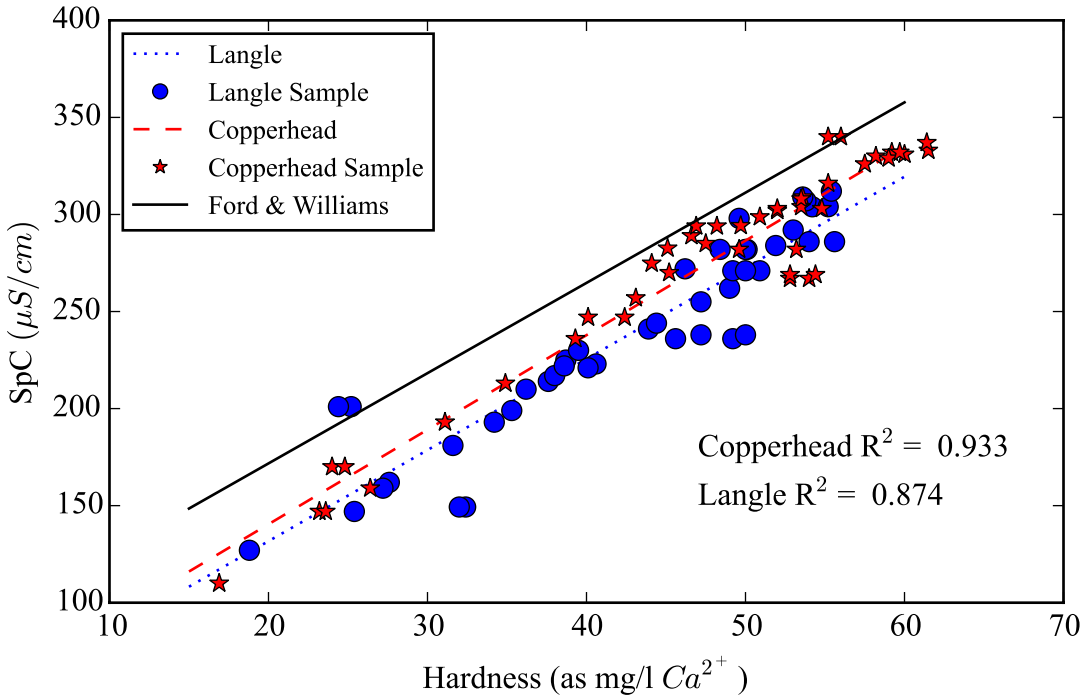

Figure 5. Specific conductance versus hardness expressed as mg L^{-1} Ca^{2+} at both Copperhead and Langle springs. Also shown, the worldwide relationship, developed by Krawczyk and Ford, 2006, between specific conductance versus total hardness (as mg L^{-1} $CaCO_3$) has been modified to represent a equivalent relationship between specific conductance versus hardness expressed as mg L^{-1} Ca^{2+}.

Temperature

The air temperatures for the study area ranged from -20°C to 36.7°C during the study period. The warmest air temperatures for the area were seen on July 10, 2013 and July 26, 2014 and the coolest on December 7, 2013 and January 6, 2014 (Fig. 6). Because there was only one winter season on record in this study, the lowest air temperatures are clustered within a 30-day period.

Water temperatures at the two springs exhibited differing behaviors, with Copperhead showing sharp changes during storm events while Langle was less responsive (Fig. 7). The water temperature for Copperhead ranged from 9.48°C to 16.5°C while Langle ranged from 10.8°C to 17.3°C. The water temperatures were highest in the fall and lowest in early spring for

both Copperhead and Langle. Monthly averaged water temperatures for both sites showed correlation to air temperature, with Copperhead being very strongly correlated and Langle being strongly correlated. Discharge also showed an inverse correlation to water temperature at both springs. Langle monthly averaged water temperature has a very strong inverse correlation to discharge while Copperhead has a strong inverse correlation (Tables 1 & 2).

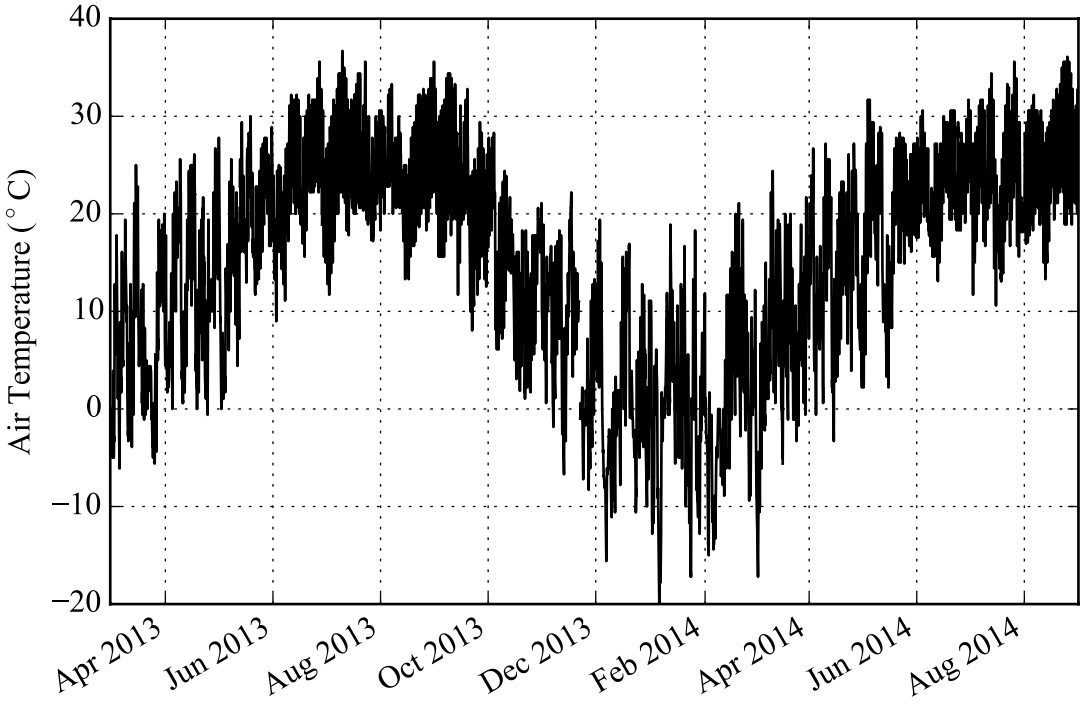

Figure 6. Air temperature measurements in degrees Celsius recorded at 1-hour resolution over the period of the study from the Northwest Arkansas Regional Airport weather station.

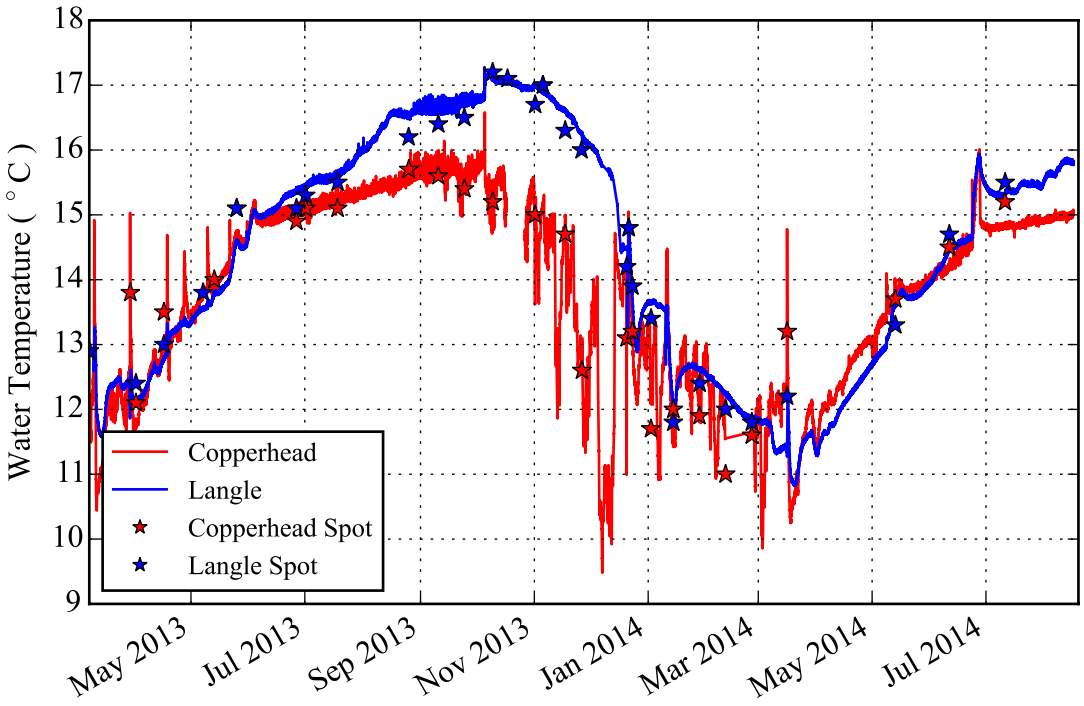

Figure 7. Water temperature measurements in degrees Celsius recorded at minute resolution over the period of the study. Also included are the field (spot) measurements.

Discharge

As precipitation monitoring was outside the scope of work for this study, the discharge measurements were used as a proxy for evaluating the influence of recharge variations. These data showed that there were three distinct climatic periods within this study. The first period, March 2013 - Mid June 2013, was a very 'wet' period with eight distinct storm events in close succession that saw an average of 6 days between events. The second period, Mid-June 2013 – Mid-December 2013, was a 'dry' period with only one distinct storm event. Lastly the remainder of the study, Mid December 2013 - August 2014, contained a mixture of dry and wet periods with eight distinct storm events with an average of 23 days between events. Copperhead was flashier in response to these storm events with more dramatic increases in discharge than Langle (Fig. 8). This was also evident in the range of discharges each spring exhibited,

Copperhead ranged from 0.045 ft^3/s – 7.58 ft^3/s while Langle's range was much less at 0.012 ft^3/s – 1.42 ft^3/s.

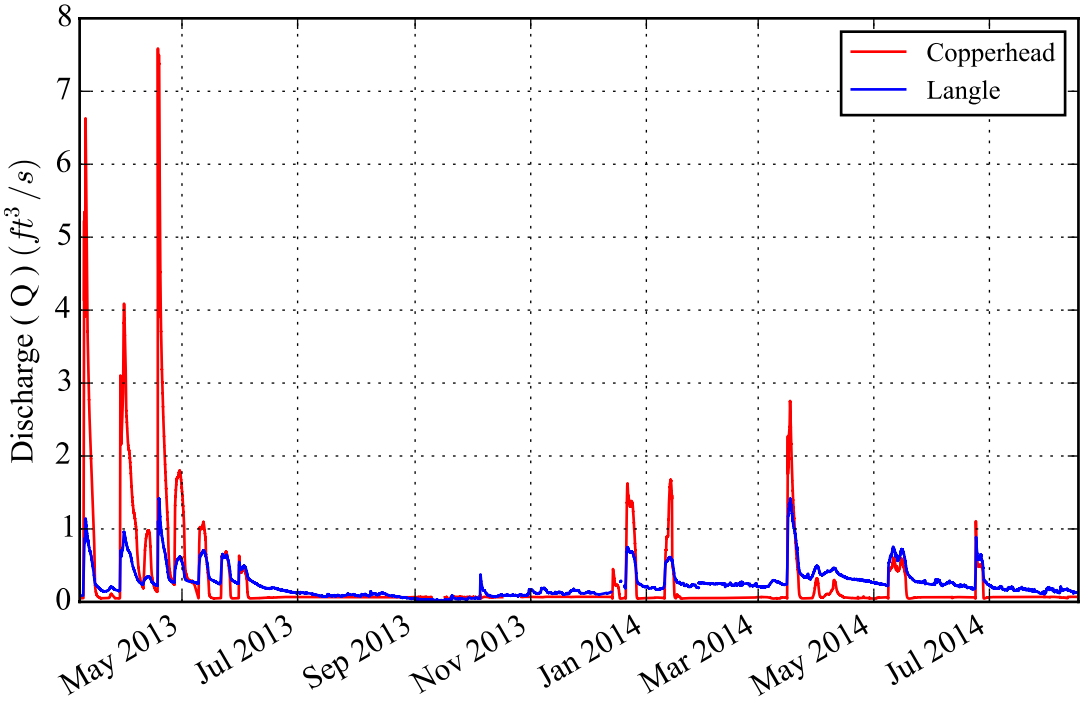

Figure 8. Discharge measurements recorded at minute resolution over the period of the study

Specific Conductance

SpC at both springs was highly variable over the study period. Copperhead maintained a higher SpC throughout a majority of the study and showed a wider range of variability, 83 – 340 µS/cm versus 94 – 299 µS/cm at Langle (Fig. 9). SpC was most variable during 'wet' periods and highest during drier periods. Monthly averaged SpC for both springs shows strong correlations to discharge (inverse), air temperature, and water temperature. Langle SpC also shows a strong correlation to P_{CO2}. SpC was most strongly correlated with discharge at both springs. (Tables 1 & 2).

	Air Temperature		CO_2		SpC		Detrended CO_2		Dissolution Rate		Discharge		Water Temperature	
	r_s	P	r_s	P	r_s	P	r_s	P	r_s	P	r_s	P	r_s	P
Air Temperature	1.000	0												
CO_2	0.517	0.028	1.000	0										
SpC	0.600	0.009	0.040	0.874	1.000	0								
Detrended CO_2	-0.051	0.842	0.618	0.006	-0.294	0.236	1.000	0						
Dissolution Rate	0.183	0.468	0.835	1.63E-05	-0.360	0.142	0.785	1.13E-04	1.000	0				
Discharge	-0.344	0.163	0.131	0.604	-0.847	9.11E-06	0.467	0.050	0.538	0.021	1.000	0		
Water Temperature	0.812	4.24E-05	0.358	0.145	0.666	0.003	-0.164	0.515	-0.026	0.919	-0.505	0.033	1.000	0

Table 1. Copperhead Monthly Average Spearman Rank-Order Correlation Coefficients with corresponding p values.

	Air Temperature		CO_2		SpC		Detrended CO_2		Dissolution Rate		Discharge		Water Temperature	
	r_s	P	r_s	P	r_s	P	r_s	P	r_s	P	r_s	P	r_s	P
Air Temperature	1.000	0												
CO_2	0.926	3.69E-08	1.000	0										
SpC	0.542	0.020	0.517	0.028	1.000	0								
Detrended CO_2	0.044	0.861	0.193	0.443	0.055	0.829	1.000	0						
Dissolution Rate	0.511	0.030	0.600	0.009	-0.333	0.176	0.135	0.593	1.000	0				
Discharge	-0.474	0.047	-0.399	0.101	-0.901	3.41E-07	-0.042	0.868	0.393	0.106	1.000	0		
Water Temperature	0.544	0.020	0.569	0.014	0.804	5.82E-05	0.026	0.919	-0.137	0.587	-0.843	1.11E-05	1.000	0

Table 2. Langle Monthly Average Spearman Rank-Order Correlation Coefficients with corresponding p values.

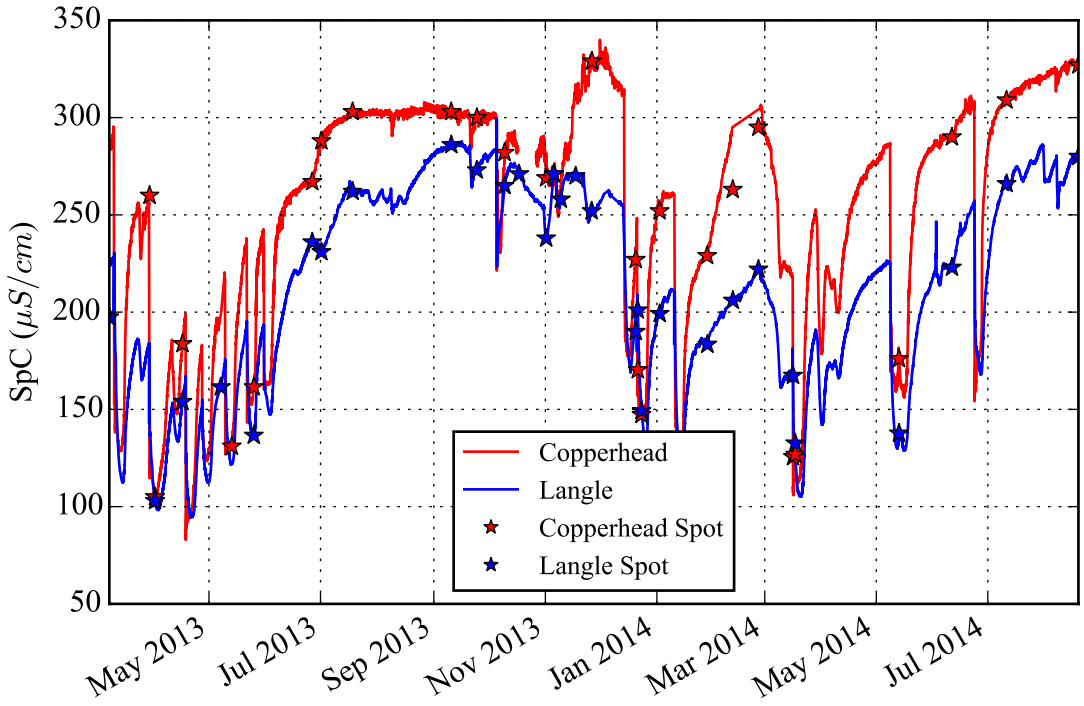

Figure 9. SpC measurements recorded at minute resolution over the period of the study. Field measurements were used to correct for drift in SpC measurements.

CO_2

Copperhead P_{CO2} ranged from 524 ppm – 20750 ppm, while Langle ranged from 1862 ppm – 23190 ppm (Fig. 10). The P_{CO2} data from both springs shows a seasonal variation with peak concentrations during the warmer periods and the lowest concentrations in the cooler periods. There is a slight temporal offset in the seasonality of the CO_2 data with peak P_{CO2} occurring just ahead of the warmest temperatures, while the lowest concentrations are just behind the coolest temperatures. Peak P_{CO2} at Copperhead was seen on June 2, 2013 and June 27, 2014, with the lowest concentrations being on seen December 30, 2013 and March 3, 2014. While peak P_{CO2} at Langle was seen on June 19, 2013 and June 26, 2014, with the lowest concentrations seen on March 7, 2013 and February 7, 2014. Over the course of the study, Langle maintained a

higher P_{CO2} for a majority of the time. During the period of March 2013 – June 2013 the P_{CO2} of both springs was very similar with a steep decline at Copperhead occurring on June 4, 2013. A similar decline is seen at Langle on June 19, 2013. These declines continue for both springs until July 14, 2013 and August 1, 2013 for Copperhead and Langle, respectively. A moderate increase for each spring occurs until August 21, 2013 (Copperhead) and August 25, 2013 (Langle) when a steady decline occurs throughout the cooler period of the study, with a few (positive increasing) variations from the general declining trend. A similar pattern occurred during 2014 although concentrations were not as similar before the drop-off, and the secondary increase is not as clearly defined.

CO_2 dynamics at each spring appeared to be controlled in general by similar factors. Among the potential controlling variables the strongest correlation to P_{CO2} was air temperature for both Copperhead and Langle (Tables 1 & 2). Monthly averaged P_{CO2} had a very strong correlation at Langle and a strong correlation at Copperhead with air temperature. Water temperature was the second strongest correlation for Langle P_{CO2}. Copperhead also shows a moderate correlation between P_{CO2} and water temperature but because the p-value is greater than the significance level of 0.05, there is inconclusive evidence about the significance of the association between the variables. For both springs, the same is true for the correlation between discharge and P_{CO2}, the p-value is greater than the significance level of 0.05.

Since air temperature has a strong correlation to CO_2 dynamics, it was necessary to examine the other possible relationships without that influence. Using a linear regression it was possible to detrend the P_{CO2} data to remove the influence of temperature (Fig. 11). The following equations were used to detrend the P_{CO2} data:

$$\text{Copperhead DT} = \text{Copperhead } P_{CO2} - \text{AT} \times 218.6 + 2435.7 \qquad (8)$$

$$\text{Langle DT} = \text{Langle } P_{CO2} - \text{AT} \times 636.5 + 2285.1 \qquad (9)$$

DT Detrended P_{CO2}

AT Air Temperature

Looking at the temperature-detrended P_{CO2} data (Fig. 12) shows there is some dependence on other controlling variables for both springs, as there is a wide range above and below the zero mark for each spring. A zero value on these graphs would indicate conditions when temperature alone can explain the P_{CO2} value. To quantify this we can use a simple measure of the fraction of the variance in the PCO_2 data that is explained by temperature (Equation 10).

$$R^2 = 1 - \frac{\text{var}(\text{Detrend } P_{CO2})}{\text{var}(P_{CO2})} \qquad (10)$$

This can range from 0 for no importance to 1 if the P_{CO2} data was purely influenced by the temperature trend. The importance of the temperature tend for P_{CO2} at Copperhead was 0.232, while at Langle it was 0.451. After temperature-detrending the P_{CO2} data another relationship was more clearly defined. At monthly resolution, temperature-detrended P_{CO2} at Copperhead has a strong correlation to discharge. This is the only relationship that can be noted through correlations, as the p-value is greater than the significance level in all other cases. Although the correlations were not as useful when looking at relationships between discharge and P_{CO2} at

Langle, visual examination of higher resolution data such as storm events may show relationships not shown with correlations.

CO_2 dynamics during individual storm events were also examined. The majority of the storms on record have higher CO_2 concentration during the falling limb of the hydrograph than during the rising limb, meaning P_{CO2} was higher after storm events. The storms depicted in Figs. 13-15 are events that occurred during wet antecedent conditions. Both springs show similar patterns but have differing ranges during these storms. For example, the storm that begins on March 29, 2013 shows the trend of each spring's P_{CO2} variations following a similar pattern of a steady increase as discharge increases but once discharge starts to decrease, P_{CO2} starts to fall ending up at a higher concentration than that at the begin of the storm. This occurs at differing P_{CO2} and discharge ranges for the two springs. For Copperhead, P_{CO2} starts at 2747 ppm and ends at 5305 ppm, but it tops out during the storm at 6882 ppm. While Langle starts at 5221 ppm, ends at 6308 ppm, and tops out at 7153 ppm. The ranges of discharge values are also different at the two springs. Copperhead has a discharge change of 0.28 ft^3/s during the storm while Langle only changes by 0.15 ft^3/s. During the study period there was one observed storm that occurred during dry antecedent conditions (Fig. 16). During this storm Copperhead and Langle P_{CO2} reacted differently than during the storms with wet antecedent conditions. For Copperhead, P_{CO2} starts at 6157 ppm and ends at 1464 ppm, but it tops out during the storm at 9080 ppm. While Langle starts at 13850 ppm, ends at 14490 ppm, and tops out at 14950 ppm. Copperhead discharge ranges over 0.06 ft^3/s during the storm while Langle ranges over 0.33 ft^3/s. In this storm, Copperhead P_{CO2} is lower on the falling limb of the hydrograph than on the rising limb, while Langle is higher on the falling limb. The real difference is in the range of variations in

discharge and P_{CO2} at the two springs. Langle has only a slight variation in P_{CO2} with a large variation in discharge where Copperhead is the complete opposite.

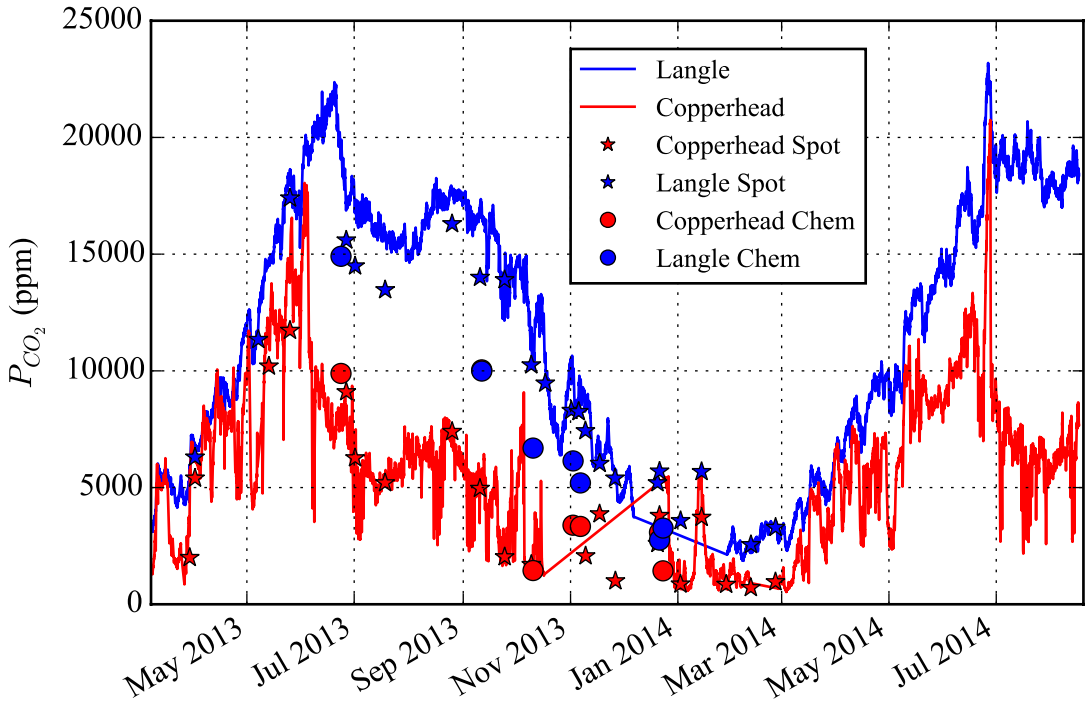

Figure 10. Partial pressure CO_2 (P_{CO2}) concentrations recorded at 1.5hr resolution at Copperhead and Langle Springs from March 2013 through August 2014. Field measurements (spot) along with chemically computed concentrations are also included for quality control. Note that some of field measurements at Langle appear to show error in the logger data, this is due to field spot measurements not having adequate time to come to equilibrium with the water.

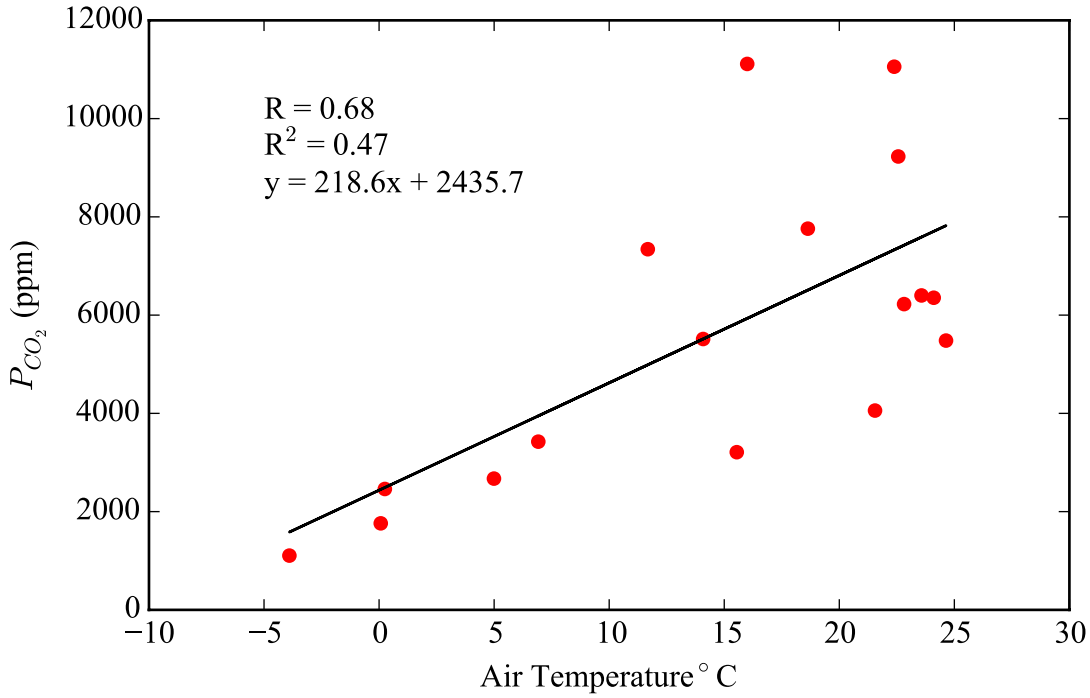

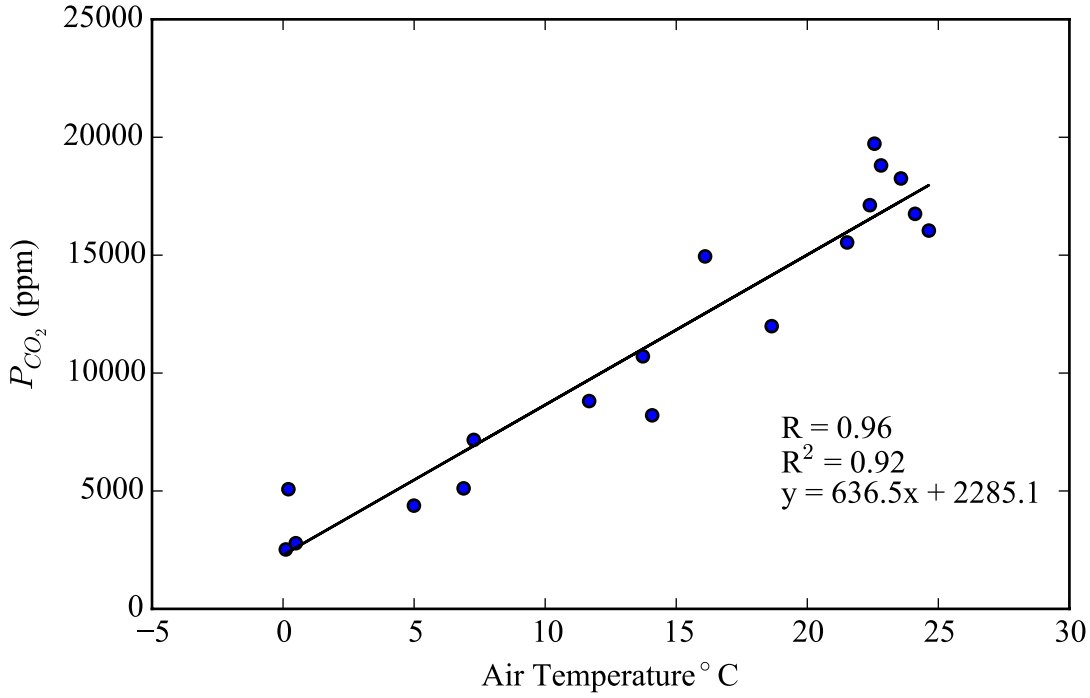

Figure 11. P_{CO2} versus air temperature at monthly resolution with temperature trend, Copperhead (Top), Langle (Bottom).

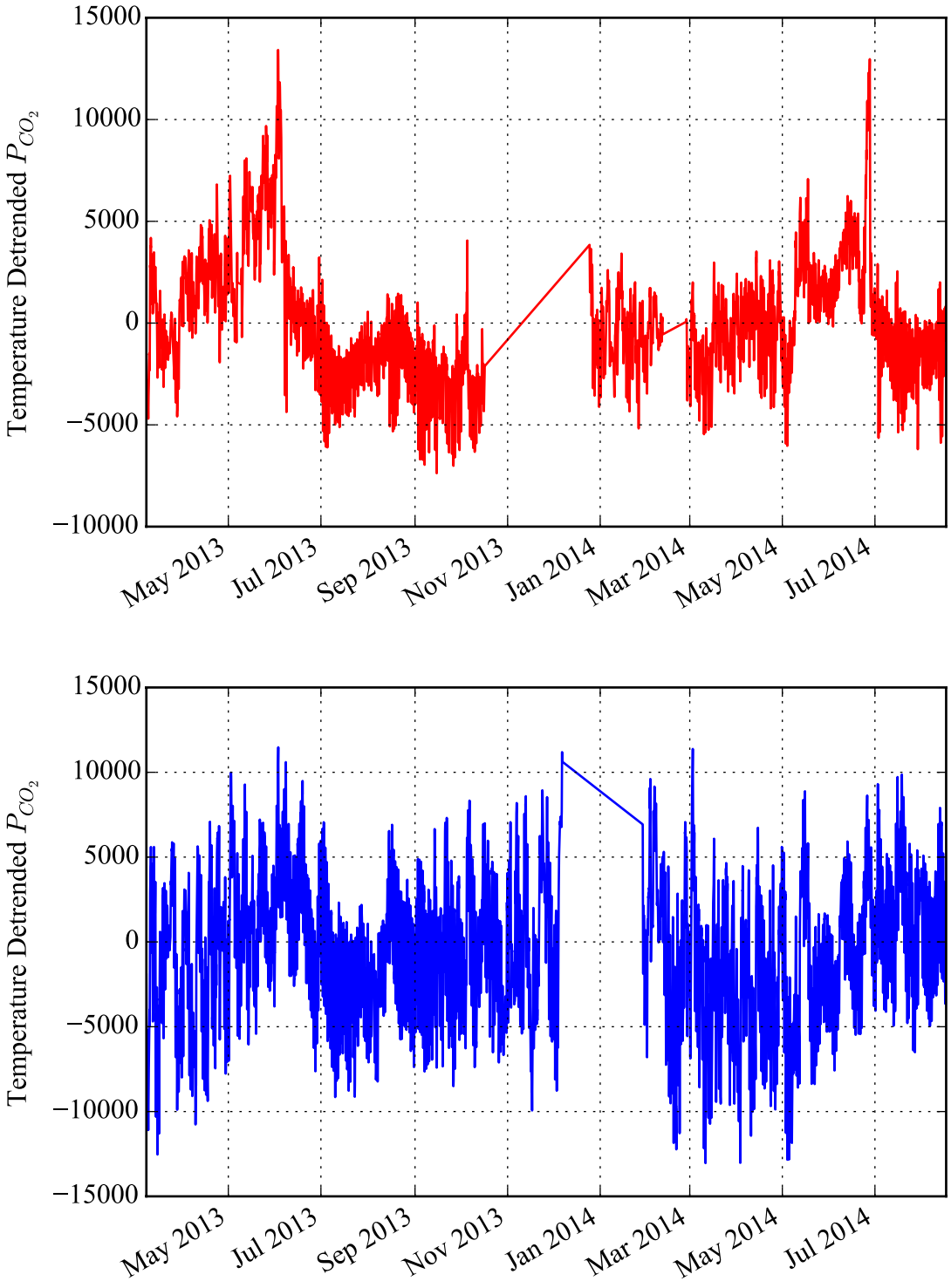

Figure 12. Temperature-detrended P_{CO2}, Copperhead (Top), Langle (Bottom).

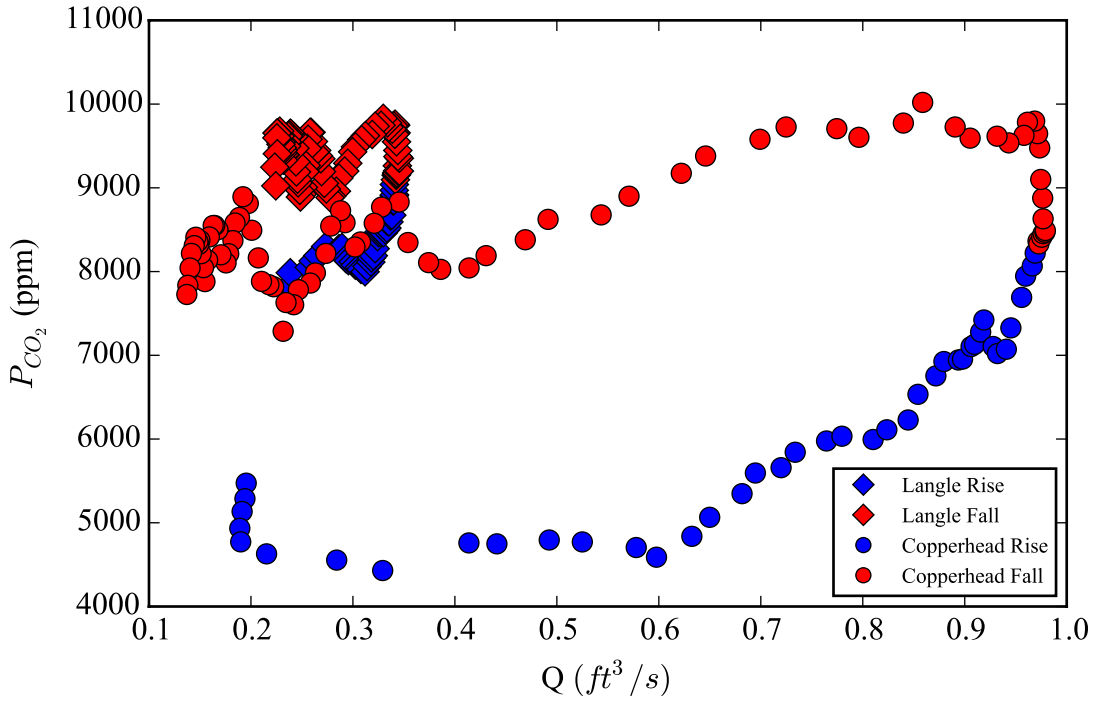

Figure 13. P_{CO2} vs. Q during a storm event that begins on 4-10-2013

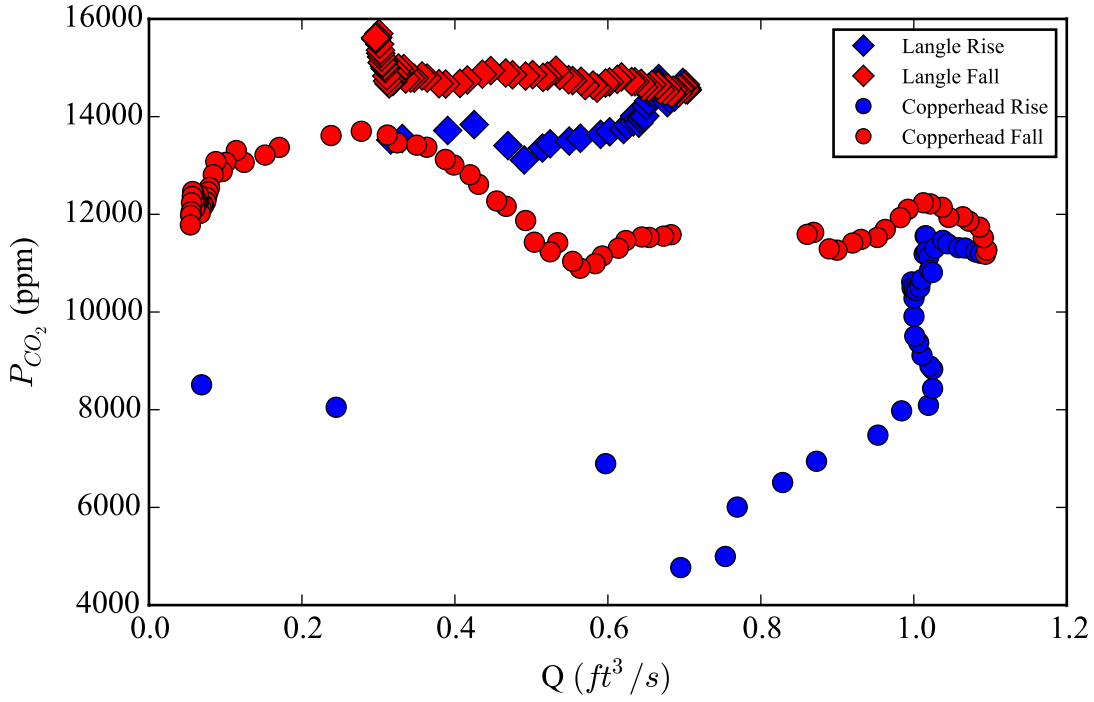

Figure 14. P_{CO2} vs. Q during a storm event that begins on 5-9-2013

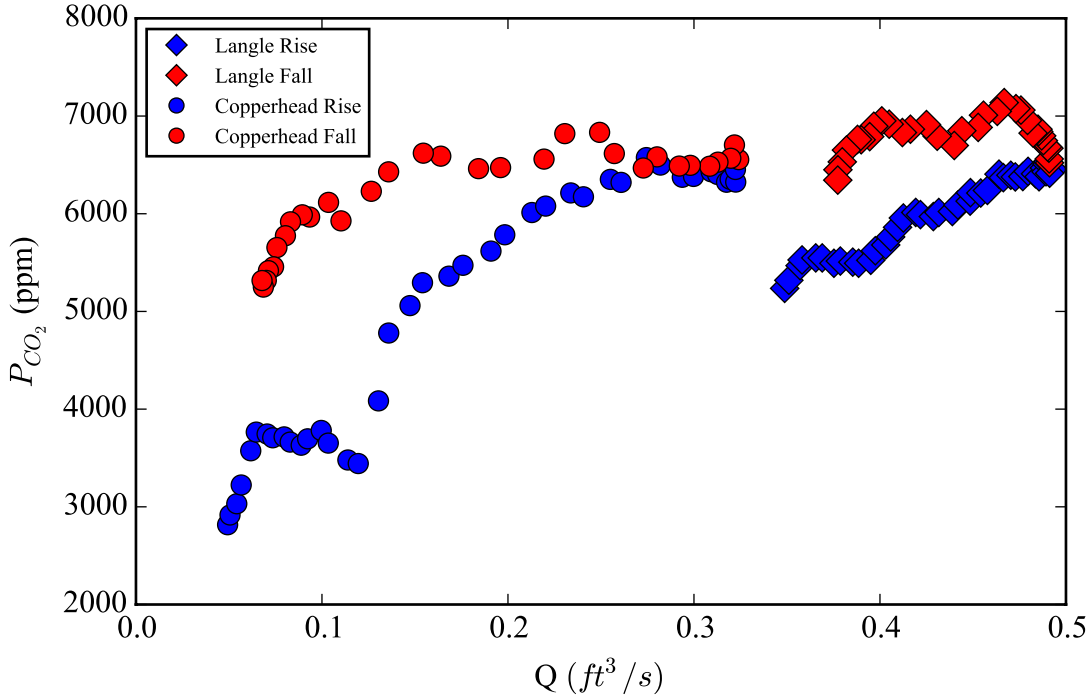

Figure 15. P_{CO2} vs. Q during a storm event that begins on 3-29-2014

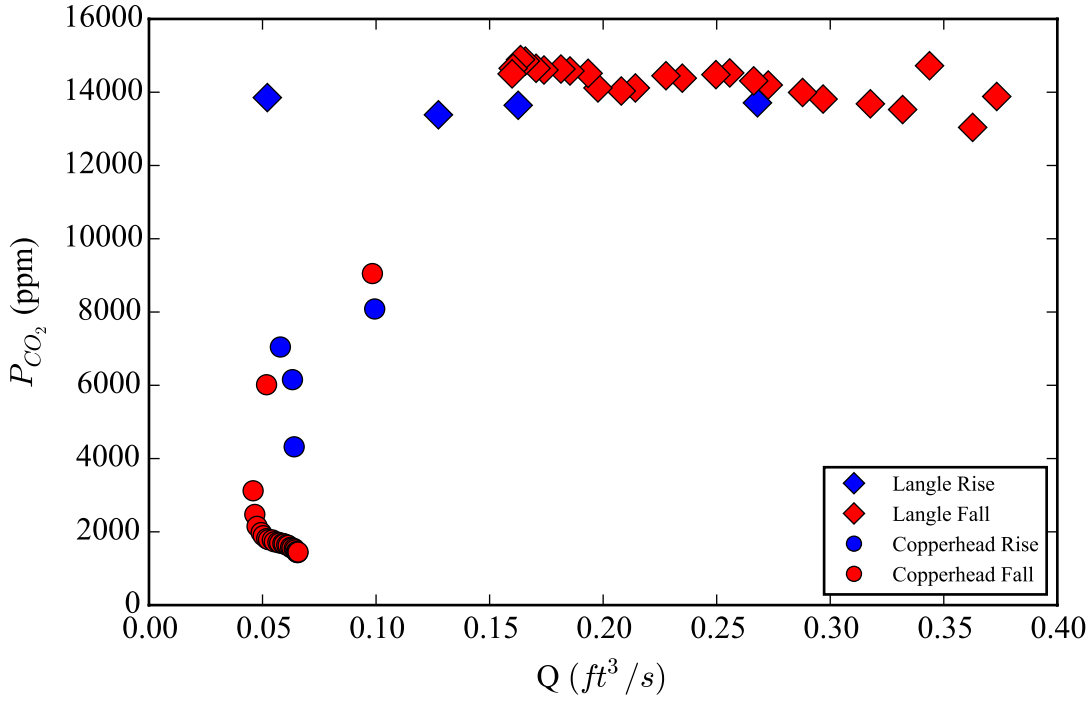

Figure 16. P_{CO2} vs. Q during a storm event that begins on 10-5-2013

Physical Dissolution Experiment and Modeled Rates

Tablets

Over the total period of exposure, tablets at Copperhead (Fig. 17) saw an average of 0.06 mm/yr of dissolution while the tablets at Langle (Fig. 18) saw an average of 0.43 mm/yr. For both springs, the highest period of dissolution occurred between May 2013 and August 2013, which was 1.03 mm/yr for Langle and 0.11 mm/yr for Copperhead. This period for both springs showed the most error in the tablet weight measurements with a standard error of the mean (SEM) of 0.32 mm/yr for Langle and a SEM of 0.07 mm/yr for Copperhead. All other tablet sets in the study had an SEM < 0.025. The larger variability during the first period could be explained by the purity of the tablets. The tablets used in this period purposely had varying levels of purity represented in the sets to test if that had any impact on the rates measured. The period with the lowest measured dissolution for Copperhead is between August 2013 and November 2013 at 0.002 mm/yr, and for Langle it was between November 2013 and February 2014 at 0.103 mm/yr.

Modeled Rates

Modeled dissolution rates for the springs over the total study period show Copperhead with an average of 0.22 mm/yr and Langle an average 0.86 mm/yr. While modeled rates without the mathematical influence of precipitation show Copperhead with an average of 0.38 mm/yr and Langle an average 0.86 mm/yr. The non-precipitation model is a more accurate representation of what actually is occurring at the springs. This is because under supersaturated conditions the PWP rate becomes negative. Mathematically these supersaturated periods show precipitation that lowers the average dissolution rate. In fact, precipitation doesn't occur until a threshold value of supersaturation is reached (Palmer, 2007), and in this case that threshold was not met.

The rates for both models are the same for Langle because the water is never supersaturated. For the majority of the study period, Langle maintained a higher dissolution rate than Copperhead (Fig. 19)

At a monthly resolution, air temperature and P_{CO2} are the strongest correlates to dissolution rate at Langle. At higher resolution, stronger correlations with SpC, and discharge are seen. Dissolution rates at Copperhead have strong relationships with P_{CO2} and discharge, P_{CO2} being the strongest (Tables 1 & 2).

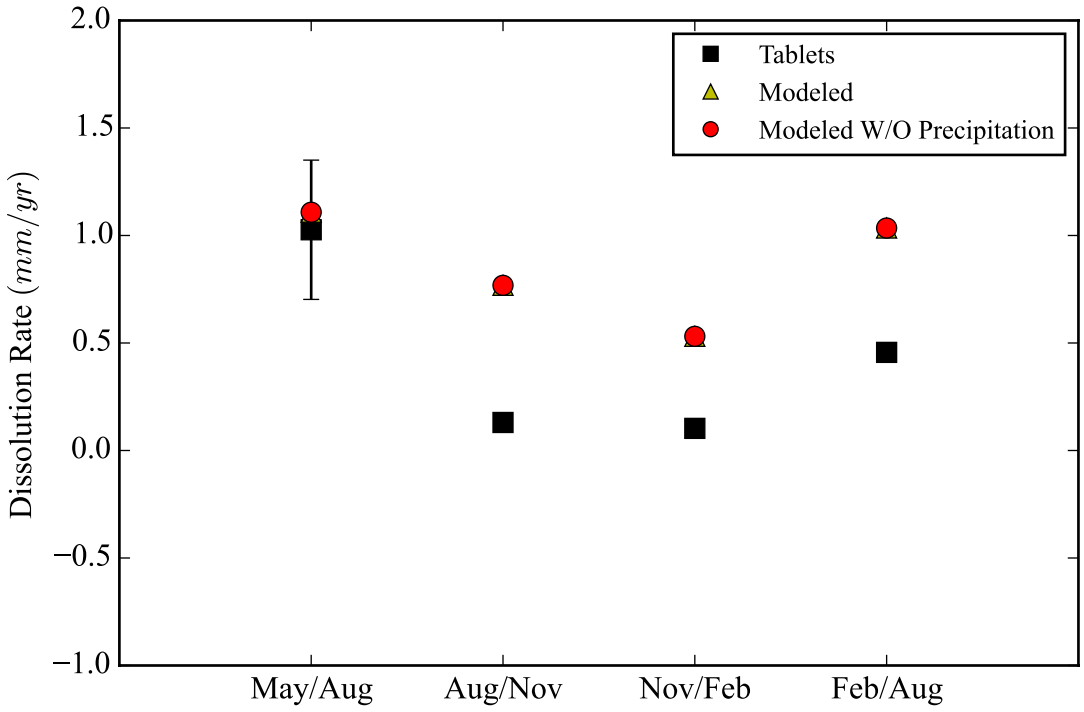

Figure 17. Dissolution rates calculated from tablets at Langle Spring over the period of the study along with modeled rates calculated from the PWP equation, with and without accounting for periods of precipitation. Note that these two values are the same as there were no periods of calculated precipitation that occurred at this site.

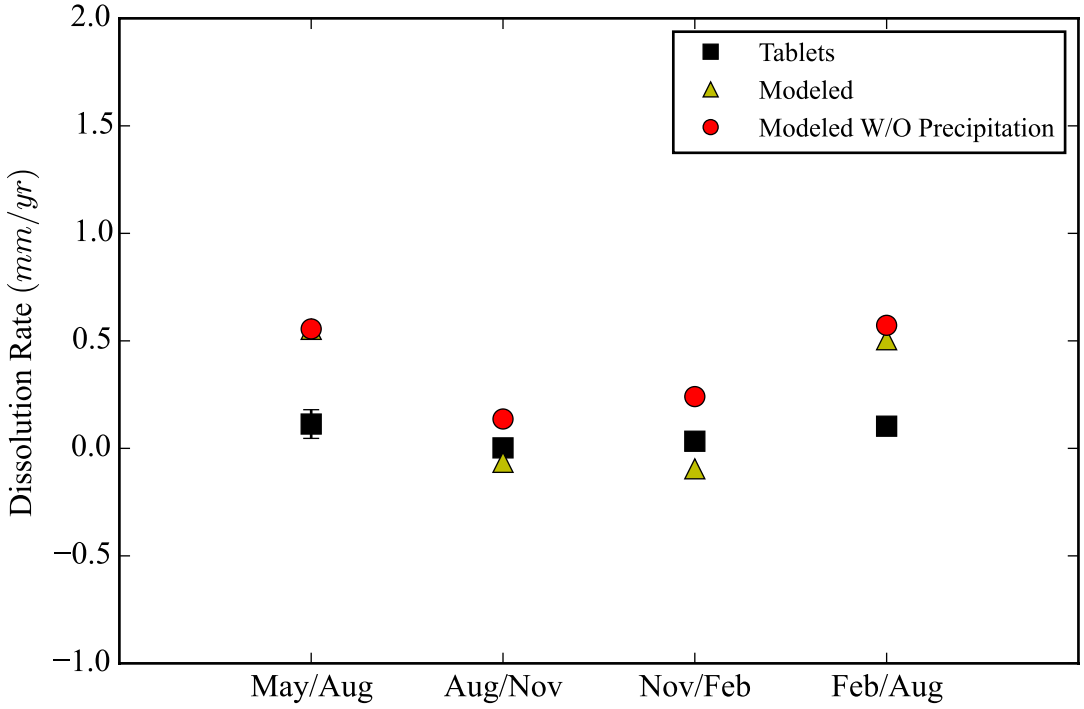

Figure 18. Dissolution rates calculated from tablets at Copperhead Spring over the period of the study along with modeled rates calculated from the PWP equation with and without accounting for periods of precipitation.

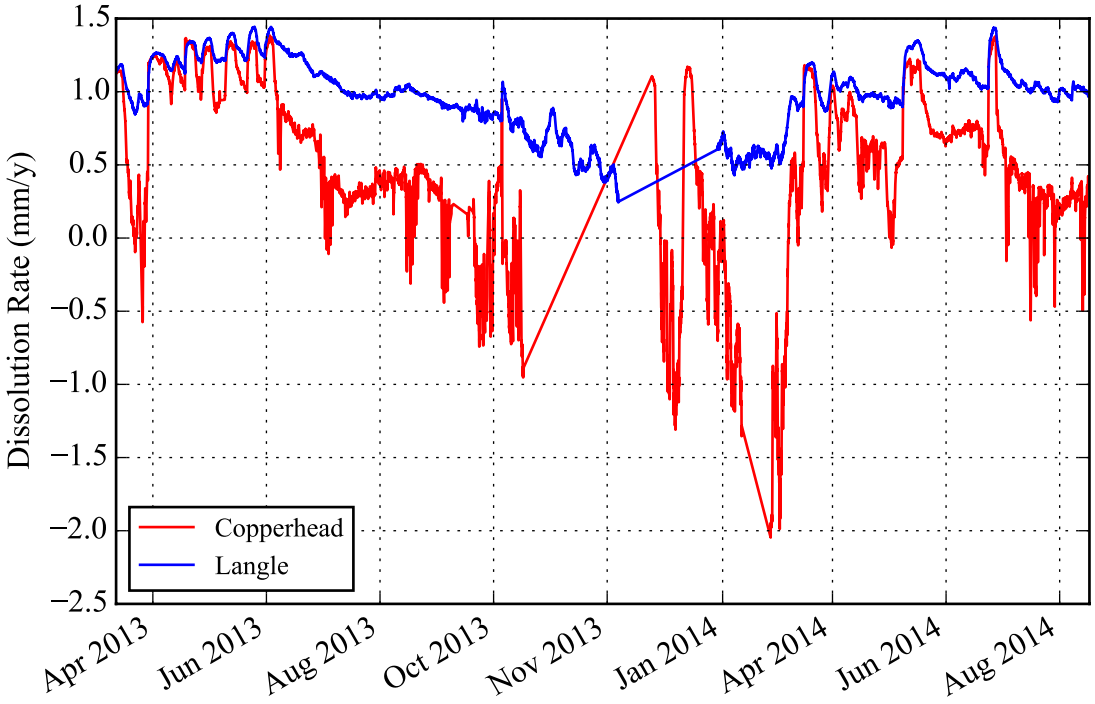

Figure 19. Dissolution rates calculated at 1.5 hr. resolution over the period of the study.

DISCUSSION

Controls on CO_2 Concentrations

Using high-resolution CO_2 data loggers at karst springs allowed for the characterization of P_{CO2} variability at sub 2-hour resolution. Using these data, it was possible to identify the main controls of that variability.

Air temperature is a strong driver for soil P_{CO2} (Reich & Schlesinger, 1992; Lloyd & Taylor, 1994; 2000; Baldini et al., 2006; Baldini et al., 2008, Knierim, 2009; Palmer, 2009; Yang et al., 2012). If soil P_{CO2} primarily controls the CO_2 dynamics in the water (White, 1988) at these springs, one might expect spring CO_2 variability to mimic variability in the soil throughout the year. Air temperature does show the strongest correlation to P_{CO2} in both springs, but not to the same degree. Langle has a near perfect relationship (r_s = .92) between P_{CO2} and air temperature, while Copperhead shows just a strong relationship (r_s = .52) when looking at monthly averaged values. However, the calculated R^2 values at both springs are sufficiently low to suggest that air temperature does not account for all the variation that is seen in either spring.

The P_{CO2} variations not accounted for by temperature could be attributed to a discharge component. The two springs tend to exhibit similar P_{CO2} during times of increased storm frequency, but as the storm frequency decreases a drop in the P_{CO2} occurs. This is first seen at Copperhead in early June 2013 and then followed by Langle in mid June 2013. This drop in P_{CO2} occurs at Copperhead after a string of smaller storm events where discharge values were similar or lower to that of Langle and a period of drought starts. The drop occurs at Langle about two weeks into the drought period. A similar drop is also seen in 2014, only slightly later in the year. An increase in P_{CO2} occurs for both springs near September 2013 when a slight increase in discharge is seen, this discharge increase was not enough to classify as a storm event. After this

slight increase there is a general decreasing trend until March of 2014 that could be caused by the decreasing temperature.

This evidence seems to point to the fact that both air temperature and discharge play a role in controlling P_{CO2} at these springs. Air temperature is the driving force of the production and availability of P_{CO2} that is incorporated into the springs, but discharge acts as a limiting factor. During the warmer months of 2013 there are high temperatures, which should result in elevated levels of P_{CO2}. However, a drop in P_{CO2} occurs due to a period of low discharge. This could be explained via several mechanisms: 1) a lack of water being flushed through the high P_{CO2} soil system, 2) a lack of water that reduces the production of P_{CO2} the soil microorganisms, or 3) increased soil degassing to the atmosphere during dry conditions.

The two springs show somewhat similar CO_2 dynamics, as well as similar controls on variability. However, there are also important differences between the two springs. Similar seasonal pattern are seen at both springs, with higher concentrations during the warmer months and lower concentrations during the cooler months, but there are extend periods of time when the P_{CO2} differs greatly between the springs. This leaves some question as to what else could be individually controlling P_{CO2} at the two springs. To explore this question, the percent difference in the springs P_{CO2} was examined, quantified as (Equation 11).

$$\text{Percent Change } P_{co2} = \frac{\text{Copperhead } P_{co2} - \text{Langle } P_{co2}}{\text{Langle } P_{co2}} \times 100 \qquad (11)$$

It is clear that during 'wet' periods the percent difference between the two springs is much less than during dry periods (Fig. 20).

The greatest difference in P_{CO2} between the two springs occurs when discharge at Copperhead falls below 0.06 ft^3/s. At higher discharges the difference between the two springs starts to diminish. This may indicate degassing occurring within the conduit system at Copperhead at low discharges. As Copperhead is the overflow spring in the system, situated at a higher elevation, it receives less of the base flow for this basin. At low discharges, water levels in the system may fall below a point that allows for direct atmospheric interaction with the conduit system and consequent degassing of the elevated P_{CO2}. This could explain observed differences between the P_{CO2} patterns at the two springs. Alternatively, at varying discharge ranges the source of the water for each spring could change substantially causing a similar effect. However in that case it would still imply that the water in Copperhead, even if it is mostly coming from some other source, has had more chance to de-gas.

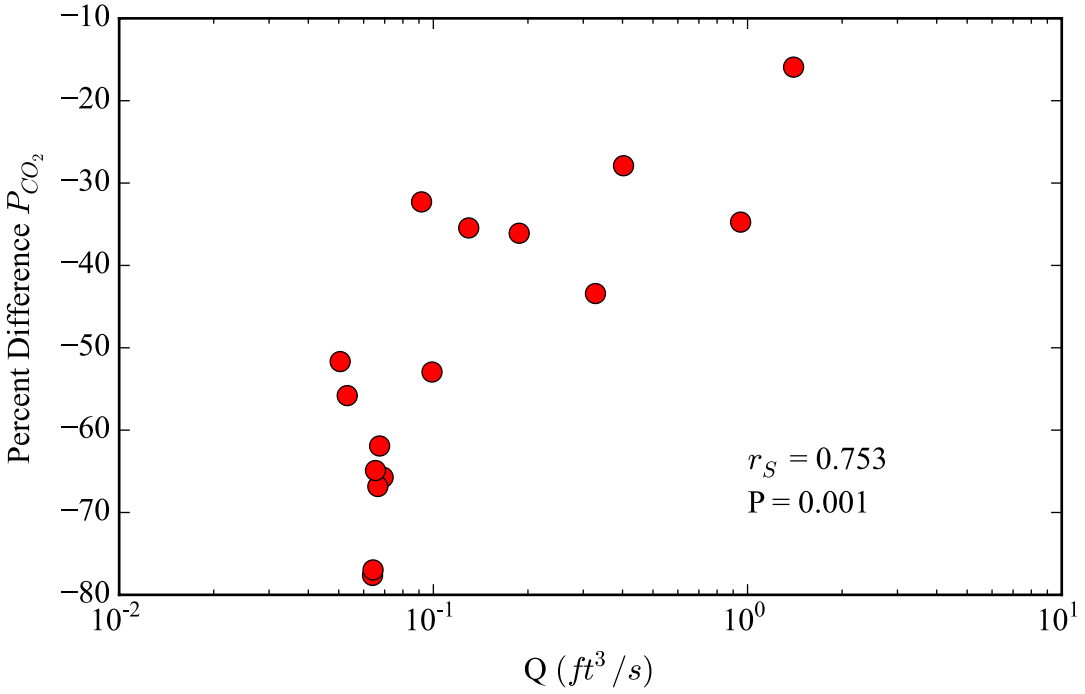

Figure 20. Copperhead and Langle P_{CO2} percent difference versus Copperhead discharge measurements at monthly resolution.

Controls on Modeled Dissolution Rates

Utilizing the high-resolution CO_2 data allowed for the sub 2-hour resolution of calculated dissolution rates in this study. As with P_{CO2} some periods of data were missing but it was possible to identify the main controls of dissolution rates. Dissolution rate variability can be controlled by a variety of factors: the aggressiveness of the water, hydraulics, rock type, and temperature (Palmer, 2009). Mathematically the modeled dissolution rates for this study are dependent on three variables, Ca^{2+} concentration, water temperature, and P_{CO2}.

The Ca^{2+} concentrations that are used for the calculations were computed values based on a linear regression between Ca^{2+} concentrations and corresponding SpC values measured from water samples at each spring. Consequently, the calculated Ca^{2+} concentrations display the same

strong correlation with discharge as SpC does. This relationship shows higher discharges result in lower Ca^{2+} concentrations and visa versa. So, looking at the relationship between dissolution rate and Ca^{2+} concentration in general (Fig. 21), the higher the Ca^{2+} concentration the lower the dissolution rate. This results because the aggressiveness of the water is reduced with higher dissolved loads (Palmer, 1999). Water temperature shows no significant correlation to the dissolution rate variation at either spring. Both springs show a strong correlation between P_{CO2} and dissolution rates (Fig. 22), suggesting that CO_2 dynamics are an important driver of dissolution rate variability. As stated previously, P_{CO2} at these two springs is controlled in part by air temperature and discharge.

Dissolution rates at the sites have a similar long-term pattern as P_{CO2}. The springs have similar dissolution rates during times of increased discharge (Fig. 23). During periods with high discharge higher dissolution rates occur, and when discharge decreases dissolution rate also decreases. Dissolution rates are also higher in the warm period and lower in the cooler period, which aligns with the conclusion that CO_2 dynamics are an important driver of dissolution rate variability.

Although dissolution rates show strong correlations with multiple variables including: Ca^{2+} concentrations, discharge, and P_{CO2}. CO_2 dynamics are the strongest driving force in the dissolution rate variations at Copperhead, while the influence of Ca^{2+} concentration and discharge is secondary. The controlling factor of dissolution rate variations at Langle is not as clear looking when looking at the correlations. Correlations at Langle with all three variables are similar.

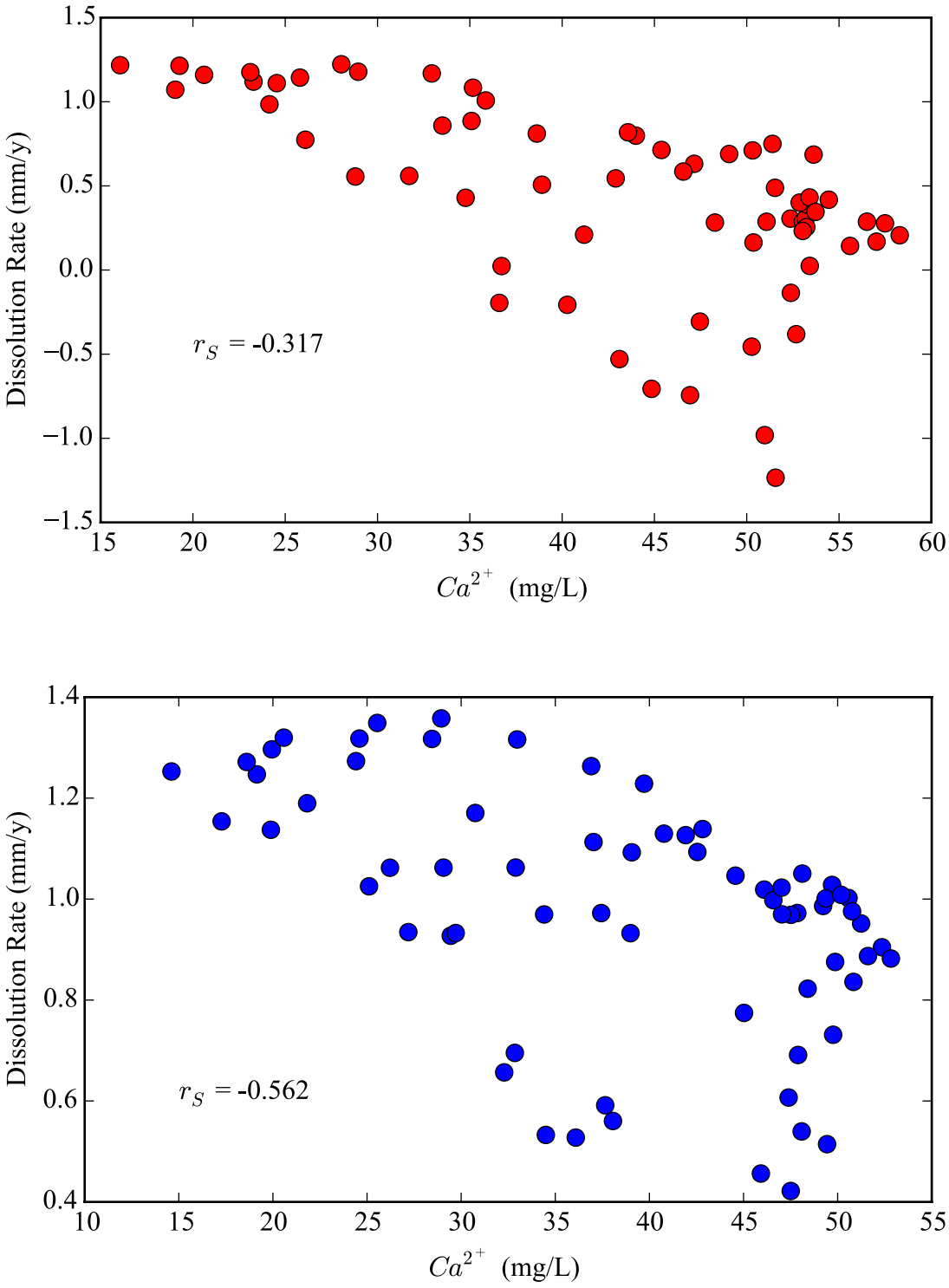

Figure 21. Ca^{2+} concentrations versus dissolution rate at weekly resolution, Copperhead (Top), Langle (Bottom).

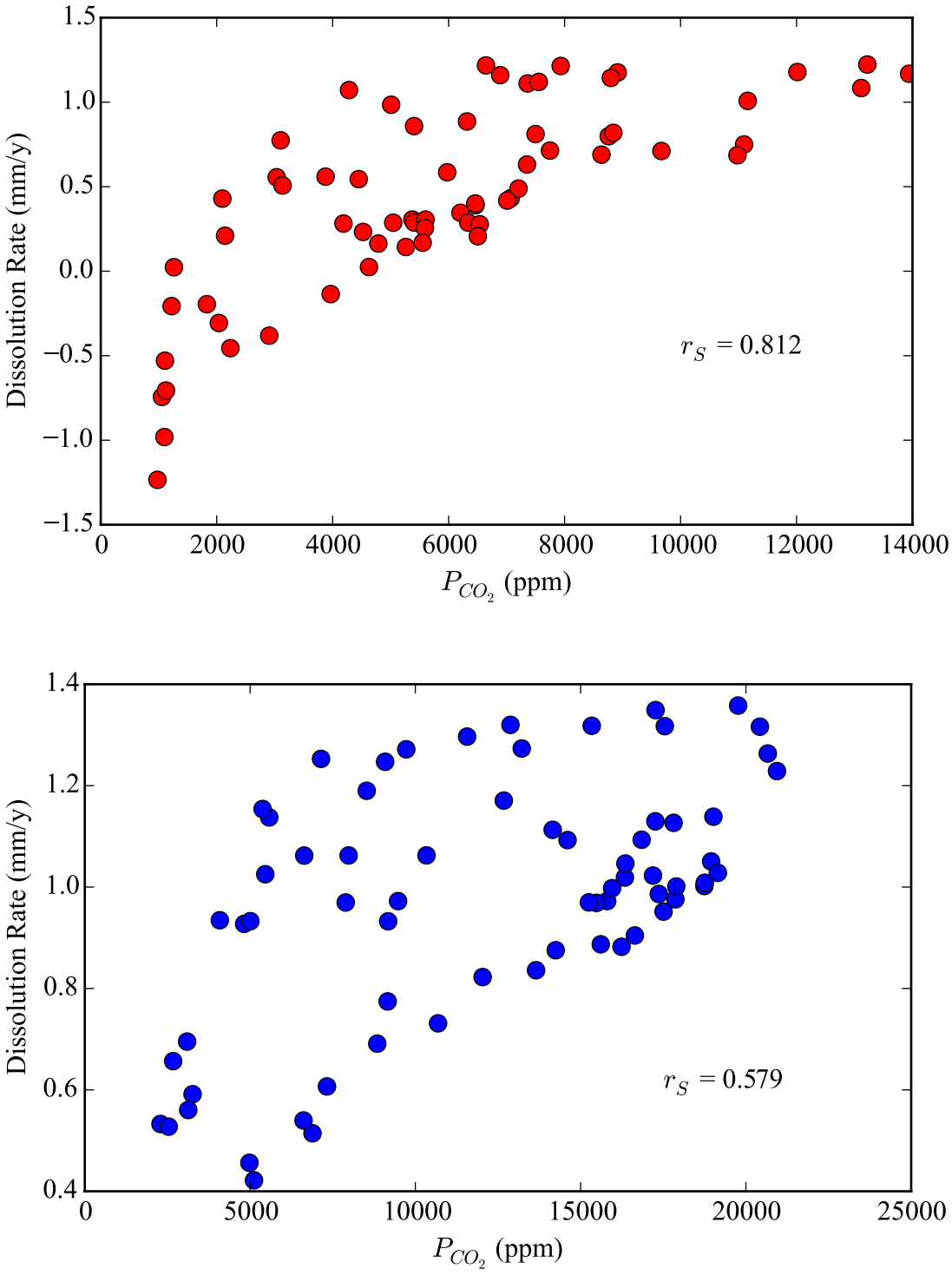

Figure 22. P_{CO2} versus Dissolution rates at weekly resolution, Copperhead (Top), Langle (Bottom).

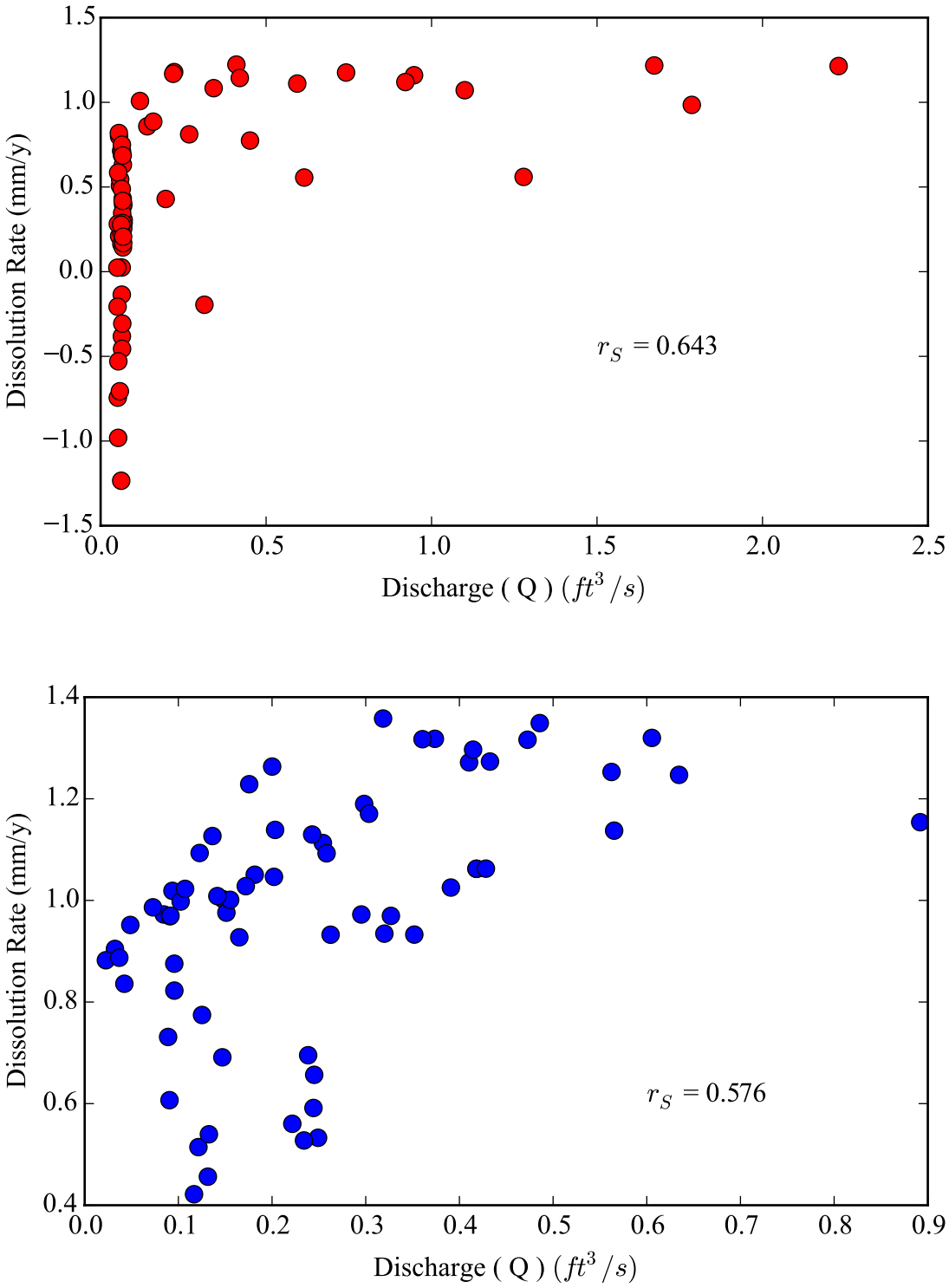

Figure 23. Discharge versus dissolution rates at weekly resolution, Copperhead (Top), Langle (Bottom).

Measured Dissolution Rates vs. Modeled Dissolution Rates

Conducting a physical dissolution experiment along side continuous measurements of physical and chemical water parameters enabled a side-by-side comparison of modeled dissolution rates vs. measured dissolution rates. Field measured rates confirmed that Langle experienced more dissolution over the period of the study as seen in the modeled dissolution rates. Copperhead saw an average of 0.06 mm/yr of dissolution in the field while the models showed rates of 0.38 mm/yr. Langle saw an average 0.43 mm/yr of dissolution in the field while the models showed rates of 0.86 mm/yr. In both sites, the models over predicted dissolution rates, at Copperhead it was by 530 % while at Langle it was 100 %. Looking at the modeled rates versus measured rates (Fig. 24) shows that while the modeled rates were not precise in their predictions they were able to identify the general trend. The relationships between modeled and observed are relatively well fit by a straight line, especially at Copperhead. However, more data would be needed to produce a robust statistical comparison between the modeled and observed rates. The over prediction of the model rates possibly stem from the fact that the dissolution models are for pure calcite whereas the tablets were limestone. It has been shown that the rates of the reaction can be reduced by impurities in the rock, which inhibit the surface reaction causing rates to be lower (Dreybrodt & Eisenlohr, 2000). Also, our model assumes that the rates are limited by the surface reaction rather than transport. While this is the prediction of the theory under turbulent flow conditions, the exact importance of transport is uncertain (Covington, 2014). The better model fits at Langle could be explained by either of these effects. The influence of impurities is stronger near saturation, where Copperhead spent most of its time. Additionally, water is more ponded and has lower velocities at the measurement site at Copperhead and the possibility of transport-limited rates is higher.

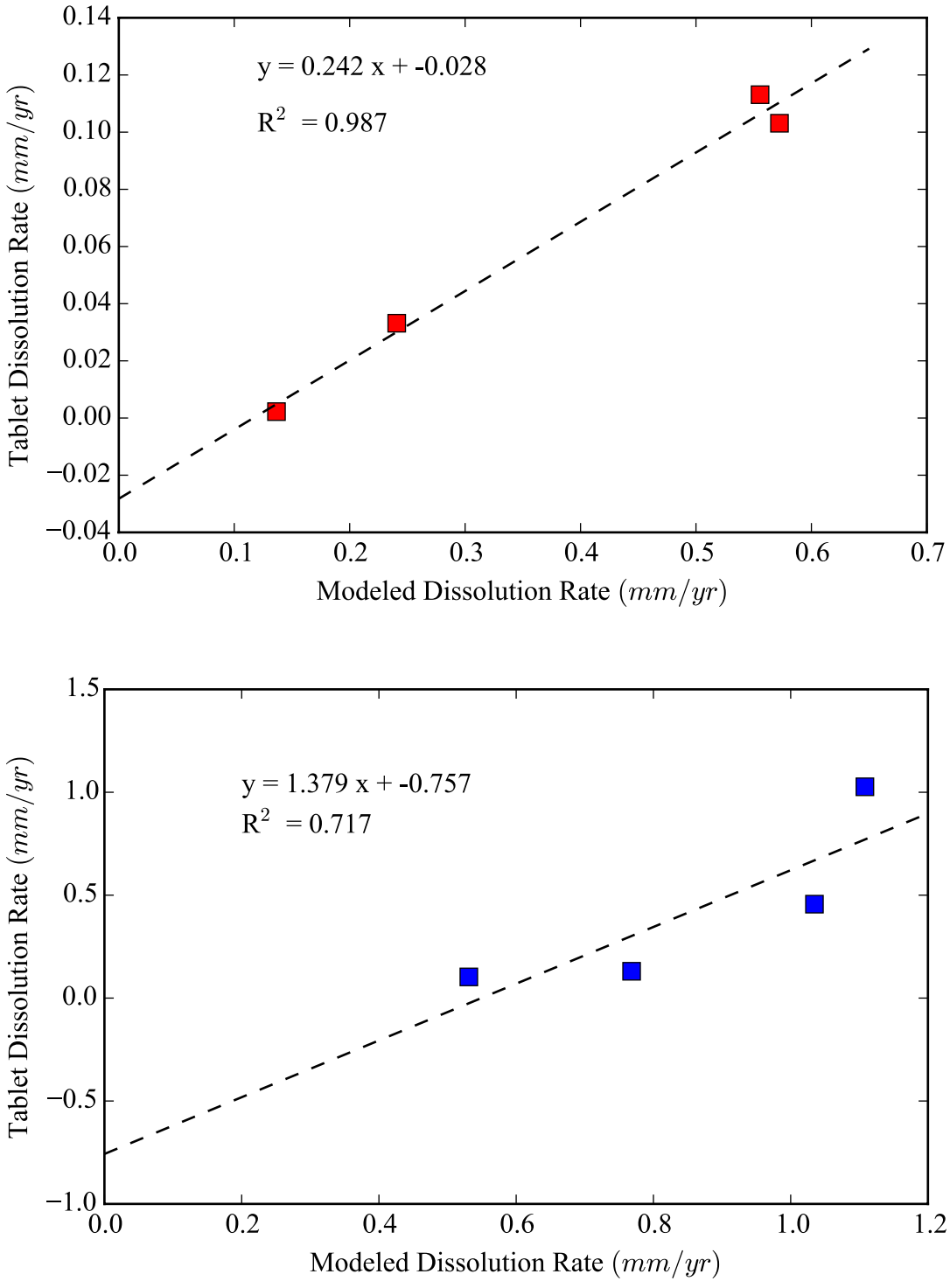

Figure 24. Modeled dissolution rates versus tablet dissolution rates, Copperhead (Top), Langle (Bottom).

CONCLUSIONS

Historically when studying karst springs a majority of the physical and chemical parameters could be measured and recorded at high-resolution. This study combines measurement of those parameters with high-resolution measurements of P_{CO2}, numerical modeled dissolution rates, and measurements of onsite dissolution rates. This allowed for characterization of the potential controlling variables of the dissolution rate at the two-karst springs.

The characterization of the springs' variability was done through the monitoring of these variables over a period of 526 days, which allowed for the identification of trends and patterns within the data from storm event scales to seasonal scales. Through the use of dedicated probes attached to data loggers at each spring location, high-resolution measurements of SpC, stage, water temperature, and P_{CO2} were recorded. Measurements of SpC, stage, and water temperature were recorded at one-minute resolution, while the P_{CO2} was recorded at 1.5-hour resolution. Air temperatures for the sites were externally sourced at one-hour resolution. Using the high-resolution data, dissolution rates were estimated for each spring from available chemical models. Along side the high-resolution monitoring of physical and chemical parameters, a physical dissolution experiment was conducted at each spring. This consisted of using weight loss in limestone tablets that were placed at each spring to quantify dissolution rates.

Using correlation coefficients and qualitative observation of time series patterns, relationships were identified for both springs in the study. P_{CO2} at both springs showed to have strong relationships with air temperature and discharge. Air temperature is a strong influence on soil CO_2 concentration, which in turn controlled the water P_{CO2}. Peak concentrations occurred during the warmer periods and the lowest concentrations in the cooler periods. The influence of

discharge is two-fold. First, there was a positive correlation between discharge and P_{CO2}. Alternatively discharge can also influence dissolved load via dilution. In periods of low flow, higher ionic concentrations in the water a limited dissolution.

Having identified the controls of P_{CO2} it was then possible to see what effect P_{CO2} variation had on dissolution rate variations. Modeled dissolution rates for the two springs shared strong similarities with the temporal patterns of P_{CO2}. This is perhaps not surprising since CO_2 plays a vital role in the karst dissolution process. Along with P_{CO2}, dissolution rates show strong correlations with multiple variables, including Ca^{2+} concentration and discharge. However, these are both secondary factors in comparison to CO_2. The modeled rates calculated for the sites were then compared with the rate measured from the tablets. This comparison showed that while the models generally overpredicted the rates, they matched the general trends in dissolution rates over time.

In order to more fully understand the effect of natural variations on dissolution rates, longer term monitoring should be used. This year and half study was able to capture differing seasonal patterns between the years on record, as one year was much wetter than the other and had much higher frequency of storm events. If discharge were truly controlling factor on dissolution rates, it would suggest that changes in the climate would result in differing dissolution rate trends and patterns. This study provides some evidence for this effect. The two years on record exhibit two differing climatic periods. With one year having a group of storms in a short period of time and mostly dry for the rest of the year causing dissolution rates to be relatively high and similar at both springs for the wetter periods and lower and different during the dryer periods. While the second year has storms more evenly spaced throughout that shows a

similar pattern but has less variations between events. But with longer term monitoring this effect may be more pronounced.

The use of high-resolution P_{CO2} monitoring allowed for high resolution modeled dissolution rate calculations. This in turned allowed for dissolution rate characterization that showed how the variability of natural waters effect dissolution rates over time.

References

Al-Rashidy, S.M., 1999, Hydrogeologic Controls Of Groundwater In The Shallow Mantled Karst Aquifer, Copperhead Spring, Savoy Experimental Watershed, Northwest Arkansas [M.S.Thesis]: Fayetteville, University of Arkansas, 124 p.

Atkin, O. K., Edwards, E. J., Loveys, B. R., 2000, Response Of Root Respiration To Changes In Temperature And Its Relevance To Global Warming: New Phytologist, v. 147, p. 141-154.

Baldini, J. U.L., Mcdermott, F., Hoffmann, D. L., Richards, D. A., And Clipson, N., 2008, Very High-Frequency And Seasonal Cave Atmosphere PCO_2 Variability: Implications For Stalagmite Growth And Oxygen Isotope-Based Paleoclimate Records: Earth And Planetary Science Letters, v. 272, p. 118-129.

Baldini, J.U.L., Baldini, L.M., Mcdermott, F., And Clipson, N., 2006, Carbon Dioxide Sources, Sinks, And Spatial Variability In Shallow Temperate Zone Caves: Evidence From Ballynamintra Cave, Ireland: Journal Of Cave And Karst Studies, v. 68, p. 4–11.

Bolyard, S., 2007, Hydrogeology and geochemical processes and water-quality evolution related to the Parsons Landfill near the Beaver Reservoir Area, Arkansas [M.S. Thesis]: Fayetteville, University of Arkansas, 69 p.

Brahana, J.V., Hays, P.D., Kresse, T.M., Sauer, T.J., and Stanton, G.P., 1999, The Savoy Experimental Watershed–Early Lessons for Hydrogeologic Modeling From a Well-Characterized Karst Research Site, in Proceedings, Karst Modeling, Karst Waters Institute: Charlottesville, Virginia, p. 247–255.

Brahana, Van, 2011, Ten relevant karst hydrogeologic insights gained from 15 years of in situ field studies at the Savoy Experimental Watershed; in Kuniansky, E.L., ed., U.S. Geological Survey Karst Interest Group Proceedings, Fayetteville, Arkansas, April 26-29, 2011, U.S. Geological Survey Scientific Investigations Report 2011-5031, p. 132-141.

Brooks SM, Whitaker F.F., 1997, Co-Evolution Of Early Diagenesis And Vadose Zone Hydrology Of Holocene Carbonate Sands: Earth Surface Processes And Landforms, v. 22, p. 45–58.

Chitsazan, M., 1980, Hydrogeologic evaluation of the Boone-St. Joe Aquifer [M.S. Thesis]: Fayetteville, University of Arkansas, 140 p.

Covington, M.D., Gulley, J.D., and Gabrovsek, F., in press, Natural variations in calcite dissolution rates in streams: controls, implications, and open questions: Geophysical Research Letters, doi: 10.1002/2015GL063044.

Covington, M.D., 2014, Calcite dissolution under turbulent flow conditions: a remaining conundrum: Acta Carsologica, v. 43, p. 195-202, doi: 10.3986/ac.v43i1.628.

Covington, M.D., Prelovšek, M., And Gabrovšek, F., 2013, Influence Of CO_2 Dynamics On The Longitudinal Variation Of Incision Rates In Soluble Bedrock Channels: Feedback Mechanisms: Geomorphology, v. 186, p. 85–95, doi: 10.1016/J.Geomorph.2012.12.025.

Dinsmore, K.J., Billett, M.F., and Moore, T.R., 2009, Transfer of carbon dioxide and methane through the soil-water-atmosphere system at Mer Bleue peatland, Canada: Hydrological Processes, v. 23, p. 330–341, doi: 10.1002/hyp.7158.

Dinsmore, K.J., Billett, M.F., Skiba, U.M., Rees, R.M., Drewer, J., And Helfter, C., 2010, Role Of The Aquatic Pathway In The Carbon And Greenhouse Gas Budgets Of A Peatland Catchment: Global Change Biology, v. 16, p. 2750–2762, doi: 10.1111/J.1365-2486.2009.02119.X.

Dinsmore, K.J., Wallin, M.B., Johnson, M.S., Billett, M.F., Bishop, K., Pumpanen, J., And Ojala, A., 2013, Contrasting CO_2 Concentration Discharge Dynamics In Headwater Streams: A Multi-Catchment Comparison: Journal Of Geophysical Research: Biogeosciences, v. 118, p. 445–461, doi: 10.1002/Jgrg.20047.

Dreybrodt, W., Eisenlohr, L., 2000. Limestone dissolution rates in karst environments. In: Klimchouk, A., Ford, D.C., Palmer, A.N., Dreybrodt, W. (Eds.), Speleogenesis: Evolution of Karst Aquifers: The National Speleological Society, Inc., Huntsville, AL, 2000.

Dugan, J.T., and Peckenpaugh, J.M., 1985, Effects of climate, vegetation, and soils on consumptive water use and ground-water recharge to the Central Midwest Regional Aquifer System, Mid-Continent United States: U.S. Geological Survey Water-Resources Investigations Report 85-4236, 77 p.

Ford, D., And Williams, P., 2007, Karst Hydrogeology And Geomorphology: West Sussex, England, John Wiley And Sons, Ltd, 562 p.

Gams, I., 1981, International Comparative Measurement Of Surface Solution By Means Of Standard Limestone Tablets, In Proceedings, International Congress Of Speleology, 8th, Bowling Green, KY. National Speleological Society, Huntsville, AL, USA, pp. 273–275.

Godsey, S., Kirchner, J., and Clow, D., 2009, Concentration–discharge relationships reflect chemostatic characteristics of US catchments: Hydrological Processes, v. 1864, p. 1844–1864, doi: 10.1002/hyp.

Groves, C., and Meiman, J., 2005, Weathering, geomorphic work, and karst landscape evolution in the Cave City groundwater basin, Mammoth Cave, Kentucky: Geomorphology, v. 67, p. 115–126, doi: 10.1016/j.geomorph.2004.07.008.

Groves, C., Meiman, J., And Howard, A.D., 1999, Bridging The Gap Between Real And Mathematically Simulated Karst Aquifers, In Proceedings, Karst Modeling, Karst Waters Institute: Charlottesville, Virginia, p. 197-202.

Hach Environmental, 2008, pH—Water Quality Sensors. Loveland, CO: http://www.hydrolab.com/Products/ph.asp.

Hope, D., Dawson, J.J.C., Cresser, M.S., And Billett, M.F., 1995, A Method For Measuring Free CO_2 In Upland Streamwater Using Headspace Analysis: Journal Of Hydrology, v. 166, p. 1–14, doi: 10.1016/0022-1694(94)02628-O.

Johnson, M.S., Billett, M.F., Dinsmore, K.J., Wallin, M., Dyson, K.E., And Jassal, R.S., 2009, Direct And Continuous Measurement Of Dissolved Carbon Dioxide In Freshwater Aquatic Systems-Method And Applications: Ecohydrology, v. 3, p. 68–78, doi: 10.1002/Eco.95.

Kling, G., Kipphut, G., Miller, M., 1991, Arctic Lakes And Streams As Gas Conduits To The Atmosphere: Implications For Tundra Carbon Budgets: Science, v. 251, p. 298–301.

Knierim, K, 2009, Seasonal Variation Of Carbon And Nutrient Transfer In A Northwestern Arkansas Cave [M.S. Thesis]: Fayetteville, University of Arkansas, 126 p.

Krawczyk, W.E., and Ford, D.C., 2006, Correlating specific conductivity with total hardness in limestone and dolomite karst waters: Earth Surface Processes and Landforms, v. 31, p. 221–234, doi: 10.1002/esp.1232.

Laubhan, A.C., 2007, A Hydrogeologic and water-quality evaluation of the Springfield aquifer in the vicinity of North-Central Washington county, Arkansas [M.S. Thesis]: Fayetteville, University of Arkansas, 182 p.

Lloyd, J., Taylor, J. A., 1994, On The Temperature Dependence Of Soil Respiration: Functional Ecology, v. 8, p. 315-323.

Neal, C, House WA, Down K., 1998, An Assessment Of Excess Carbon Dioxide Partial Pressures In Natural Waters Based On pH And Alkalinity Measurements: Science Of The Total Environment, v. 210, p. 173–185.

Palmer, A.N., 1999, Patterns Of Dissolution Porosity In Carbonate Rocks, in Proceedings, Karst Modeling, Karst Waters Institute: Charlottesville, Virginia, p. 71–78.

Palmer, A.N., 2007, Cave Geology: Dayton, Ohio, Cave Books, 454 p.

Palmer, A.N., 2007, Variations In Rates Of Karst Processes: Acta Carsologica, v.36, p.15-24.

Parse, M.W., 1995, Geomorphic analysis of the role of regolith in karst landscape development, Benton county, Arkansas [M.S. Thesis]: Fayetteville, University of Arkansas, 177 p.

Pennington, D.W., 2010, Karst Drainage-Basin Analysis Using Water-Level Data And Hydrograph Decomposition Techniques At The Savoy Experimental Watershed, Savoy, Arkansas [M.S. Thesis]: Fayetteville, University of Arkansas, 223 p.

Plan, L., 2005, Factors Controlling Carbonate Dissolution Rates Quantified In A Field Test In The Austrian Alps: Geomorphology, v. 68, p. 201–212, doi: 10.1016/J.Geomorph.2004.11.014.

Plummer, L.N., Wigley, T.M.L., Parkhurst, D.L., 1978. The kinetics of calcite dissolution in CO_2 water systems at 5° to 60 °C and 0.0 to 1.0 ATM CO_2. Am. J. Sci. 278,179–216.

Raich, J. W., And Schlesinger, W. H., 1992, The Global Carbon Dioxide Flux In Soil Respiration And Its Relationship To Vegetation And Climate: Tellus B, v. 44, p. 81-99.

Shelby, P.R., 1986, Depositional history of the St. Joe-Boone Formations of northern Arkansas [M.S. Thesis]: Fayetteville, University of Arkansas, 135 p.

Stumm W., Morgan J.J., 1995., Aquatic Chemistry: Chemical Equilibria And Rates In Natural Waters, Volume 126: New York, John Wiley And Sons.

Trudgill, S.T., 1975, Measurement Of Erosional Weight-Loss Of Rock Tablets: British Geomorphological Research Group Technical Bulletin, v. 17, p. 13-19.

Unger, T.T., 2004, Structural controls influencing groundwater flow within the mantel karst of the Savoy Experimental Watershed, Northwest Arkansas [M.S. Thesis]: Fayetteville, University of Arkansas, 130 p.

Vardy, R., 2011, Characterization of Urban Impact on Water Quality of Karst Springs in Eureka Springs, Arkansas; in Kuniansky, E.L., ed., U.S. Geological Survey Karst Interest Group Proceedings, Fayetteville, Arkansas, April 26-29, 2011, U.S. Geological Survey Scientific Investigations Report 2011-5031, p. 44–53.

White, W. B., 1988, Geomorphology and hydrology of karst terrains: New York, Oxford University of Press, 464 p.

Whitsett, K.S., 2002, Sediment And Bacterial Tracing In Mantled Karst At Savoy Experimental Watershed Northwest Arkansas [M.S. Thesis]: Fayetteville, University 0f Arkansas, 66 p.

Yang, R., Liu, Z., Zeng, C., and Zhao, M., 2012, Response of epikarst hydrochemical changes to soil CO_2 and weather conditions at Chenqi, Puding, SW China: Journal of Hydrology, v. 468-469, p. 151–158, doi: 10.1016/j.jhydrol.2012.08.029.

YSI Environmental. 2008: https://www.ysi.com/documentserver/documentserver?dociddemse36.